ORE DEPOSITS OF BUTTE, MONTANA

Mark Reed[1] and John Dilles[2]

[1]*Department of Earth Sciences, University of Oregon, Eugene, Oregon*

[2]*College of Earth, Ocean, and Atmospheric Sciences, Oregon State University, Corvallis, Oregon*

INTRODUCTION

Mining in the Butte District began in 1864 with the discovery of placer gold, which produced 75,000 oz by 1867. Prospectors quickly explored veins on the Butte Hill and staked claims by 1874, but much of the early underground mining was concentrated on silver-rich veins on the periphery of the district, and there was little production from leached gossans of vein exposures over the copper-rich center of the district. Copper ores were discovered after the Hearst Syndicate began to finance Marcus Daly in 1881. By 1884, Daly had deepened the Anaconda shaft to 180 m depth, and discovered 15- to 30-m widths of rich chalcocite copper ore on the Anaconda Vein. Initial production from the Anaconda mine averaged 12 wt% copper and 25 oz/tonne silver, and was shipped to a smelter in Swansea, Wales. In 1893, the Anaconda Company began construction of the smelter and the town of Anaconda 43 km west of Butte, together with connecting railroad lines. By 1892, Anaconda production reached 50,800 tonnes (100 million pounds) of copper, and made it the largest copper mine in the USA. Daly's Anaconda group also developed banks, power plants, water and timber supplies, and acquired many adjoining mines. In 1899, the Amalgamated Copper Company of New York acquired the Daly–Hearst interests, and following the 1886–1906 "Battle for Butte" acquired the Fritz Heinze and William C. Clark mines in 1906 and 1909, respectively. Once consolidated, the name reverted to the Anaconda Company.

The Butte production until 1955 came solely from the underground mines on the Main Stage lodes of southwest-striking Anaconda (Steward) veins and the northwest-striking Blue Veins. Production peaked during World Wars I and II and coincided with the installation of new technology in electric lighting, pumping and hoisting systems, and pneumatic drills. Underground mining reached a mile (1.6 km) depth, and Butte miners said the veins were "a mile long, a mile wide, and a mile deep." Production steadily declined following World War II when large amounts of manganese were mined. Underground block caving of low-grade copper ores in central horsetail zones was conducted from 1952 to 1962, and mining and pumping ceased in the Kelley shaft by 1982.

In 1955, Anaconda began open-pit mining of low-grade supergene-enriched copper ores along Main Stage veins in the Berkeley Pit. By 1982, mining ceased in the Berkeley, and beginning in 1980 production transferred eastward to the porphyry Cu-Mo ores of the Continental Pit. In 1976, Anaconda was purchased by the Atlantic Richfield Oil Company (ARCO), and Anaconda Butte operations ceased in 1983. The Washington Corporation purchased the Butte District in 1985 and formed Montana Resources, which in 1986 reopened production from the Continental deposit. From 1989 to 2000, Montana Resources mined there in partnership with ASARCO, and after closure from 2000–2003, has mined from 2003 to the present (Czehura, 2006). The preceding overview is largely taken from the recent review by Cathro (2009).

The Butte District is one of the largest historic producers in the USA of copper, molybdenum, and silver. Metal production through 2004, more than 95% of which was derived from the Main Stage veins, was Cu (9.775 Mt), Zn (2.226 Mt), Pb (0.388 Mt), Mn (1.678 Mt), Mo (97,447 t), Ag (20,276 t), and Au (98 t) [metric tons (t): Miller, 1973; Czehura, 2006; see table 1]. At that time, porphyry Cu-Mo resources included underground deposits beneath downtown Butte and between the Berkeley and Continental open pits as well as the Continental open pit resources being mined by Montana Resources. These constituted 5.4 Bt of rock averaging 0.46 wt% Cu, 0.033 wt% Mo, and 4.30 g/t Ag (i.e., 25 Mt Cu, 1.75 Mt Mo, and 23,000 t Ag resource); additional minor Cu-Zn-Pb-Ag resources

Table 1. Production and resources of the Butte district, Montana.

		million tonnes (Mt)	Metal Grade				Contained Metal (& Sulfuric Acid)							
			wt. % Cu	wt. % Mo	Ag (g/t)	Au (g/t)	Cu (t)	H_2SO4 (t)	Zn (t)	Mn (t)	Pb (t)	Mo (t)	Ag (t)	Au (t)
Production														
Production to 1881–2004	Czehura (2006)						*9,775,478*	*8,578,434*	*2,226,396*	*1,679,269*	*387,663*	*97,447*	*20,276*	*83*
Main Stage UG, 1881–1962	Long (1995)	168	~4.2		~80	~0.26	7,376,075						20,015	66
Berkeley OP, Super, MS, 1952–1982	Long (1995)	651	0.42		2.7	0.015	2,698,500						826	9
Total Main Stage 1881–1982	Long (1995)						*10,074,575*						*20,841*	*75*
Porphyry Ores, UG, 1952–1962	Long (1995)	30	0.99		17	0.14	297,000						510	4
Continental OP, 1973–1992	Long (1995)	85	0.4	0.04	2.4		340,000					34,000	204	
Continental OP, 2011	Montana Res						34,578					4,188	20	
Continental OP, Est 2005–2019							484,091					58,636	282	
Total Porphyry Ores							*1,121,091*					*92,636*	*996*	*4*
Total Production							***11,195,666***	***8,578,434***	***2,226,396***	***1,679,269***	***387,663***	***92,636***	***21,837***	***79***
													(702 M oz)	(2.55 M oz)
Resources														
pre-Main Stage (porphyry Cu-Mo)														
Continental OP, Protore, Dec. 2015	Czehura (2006, 2016)	960	0.21	0.032	3.18		2,016,563					307,286	2,091	
Continental OP Supergene	Czehura (2006)	459	0.48		3.11		2,203,601					0	1,428	
Pittsmont Dome, UG	Czehura (2006)	2,020	0.45	0.045	3.73		9,090,000					909,000	7,539	
Anaconda–Steward, UG	Czehura (2006)	1,957	0.6	0.028	6.22		11,743,636					548,036	12,174	
Continental OP, Est 2016–2019 depletion							*-129,091*					*-15,636*	*-75*	
Total Porphyry (less Est. 2016–2019 Prod)							***24,924,710***					***1,748,686***	***23,156***	
Main Stage Resources	Long (1995)													
Ag vein 1985	Long (1995)	10			69	0.1	0						690	
Cu veins 1979	Long (1995)	29	4.16				1,206,400							
Zn-Pb vein 1980	Long (1995)	121	0.5				605,000							
Total Main Stage							***1,811,400***						***690***	
Production + Resources														
Total Main Stage							11,885,975						21,531	
Total Porphyry							26,045,801					1,841,322	24,152	
Total Main Stage + Porphyry							***37,931,776***	***8,578,434***	***2,226,396***	***1,679,269***	***387,663***	***1,841,322***	***45,683***	***79***

Note. Abbreviations: g, gram; oz, troy ounces; M, million; t, tonne (metric ton) = 2,205 lbs.

occur in Main Stage veins (Long, 1995; Long and others, 2000; Czehura, 2006). Based on 2011 production rates, the 2005–2019 estimated production of Montana Resources from the Continental Pit exceeded 480,000 t Cu, 58,000 t Mo, and 280 t Ag. Thus, the sum of the total current resource inventory plus past production is approximately 38 Mt Cu, 1.8 Mt Mo, and 46,000 t Ag, which indicates that Butte is one of the Earth's largest deposits in all three metals (table 1).

In this chapter, we present a summary of the geology and mineral deposits of the Butte District by building on and updating the synthesis of Meyer and others (1968; cf., Lund and others, 2018). We first describe Butte's geological setting in the Boulder Batholith and present a summary of Butte District geology. The mineral deposits at Butte include the early or "pre-Main Stage" porphyry Cu-Mo ores, which are the subject of much recent scientific research using information derived from the deep drilling of the eastern part of the district (1978–1981). These ores are postdated by the famous and highly productive Main Stage polymetallic (Cu-Zn-Pb-Ag-Au) veins that are a primary example of rich Cordillera base metal lodes. Further, we review recent research and unresolved questions on the geologic origin and age of the giant Butte ore deposit.

BUTTE GEOLOGIC SETTING

Boulder Batholith

The ores of the Butte District formed in the granite of the south-central part of the late Cretaceous Boulder Batholith (fig.1; Scarberry and others, 2020) and are postdated by the Eocene Lowland Creek Volcanics (fig. 1; Mosolf and others, 2020; Smedes, 1962; Dudás and others, 2010). All the magmatism arises from subduction of the Farallon plate beneath North America. The Late Cretaceous and Eocene igneous rocks generally have calc-alkaline compositions, but the Eocene rocks have somewhat elevated potassium (Dudás and others, 2010). The initial Late Cretaceous magmatism resulted in eruption of up to 4 km thicknesses of andesite and dacite lavas and silicic ignimbrites of the ~86 to 82 Ma Elkhorn Mountain Volcanics (Smedes, 1966; Rutland and others, 1989; Mahony and others, 2015; Olson and others, 2016), followed by the generally younger ~83 to 76 Ma polyphase Boulder Batholith (Tilling, 1964; Smedes and others, 1988; du Bray and others, 2012). The Boulder Batholith intruded the Elkhorn Mountain Volcanics and includes a series of early satellite intrusions of granodiorite, granite, and diorite and the late intrusion of Butte Granite that constitutes about 80% of the batholith (Scarberry and others, 2020). Mineralization is widely distributed throughout the Boulder Batholith and includes porphyry Cu-Mo mineralization drilled in ~1980 by Exxon Minerals Company in the Wickes area, centered on ~82 Ma porphyry intrusions (Sillitoe and others, 1985; Olson and others, 2017; Gammons and others, 2020), the Turnley Ridge porphyry prospect near Elkhorn, gold–telluride mineralized breccia and veins at the Golden Sunlight mine, and polymetallic Pb-Zn-Ag-Cu-Au veins with ages of 74–75 Ma in the Boulder Batholith and with Elkhorn Mountain volcanic rock exposures between Wickes–Basin–Boulder and Helena–Townsend (Lund and others, 2007; du Bray and others, 2012; Olson and others, 2016). The gold–telluride mineralized breccia and veins at the Golden Sunlight mine are associated with ~84–82 Ma porphyry intrusions 5 km southeast of the main batholith (DeWitt and others, 1996; Oyer and others, 2014; J.H. Dilles, unpublished data).

The Butte mineralization is distinctly younger than the Boulder Batholith by more than 8 m.y., with the possible exception of some peripheral veins (Lund and others, 2018). Radiometric dates (fig. 2) of molybdenite and wall-rock alteration minerals in the Butte copper ores are 66 to 61 Ma (Snee and others, 1999; Martin and Dilles, 2000), overlapping with intermingled porphyry intrusions that are 67 to 61 Ma in age (Lund and others, 2002, 2018). The Butte porphyry intrusions are the only known intrusions and hydrothermal mineral deposits in the 67–61 Ma period in southwest Montana or central Idaho (Lund and others, 2007; du Bray and others, 2012). The porphyries are at least 8 m.y. younger than the Butte Granite and contain xenocrystic zircons derived from partial melting of the Butte Granite.

The Lowland Creek Volcanics overlie the Boulder Batholith in erosional unconformity, and consist of rhyolite ignimbrites, dacite lavas, and caldera–vent complexes ranging from 52 to 48 Ma (Smedes 1962; Dudás and others, 2010). The Lowland Creek Volcanics are poorly mineralized near Butte, but regionally Eocene deposits include the Heddleston porphyry Cu-Mo deposit, large epithermal Au-Ag deposits at MacDonald Gold and Montana Tunnels deposits, and numerous smaller veins and polymetallic ores. Eocene ore deposits are widespread in the Absaroka and Challis Volcanics in southwest Montana and central Idaho (Lund and others, 2007).

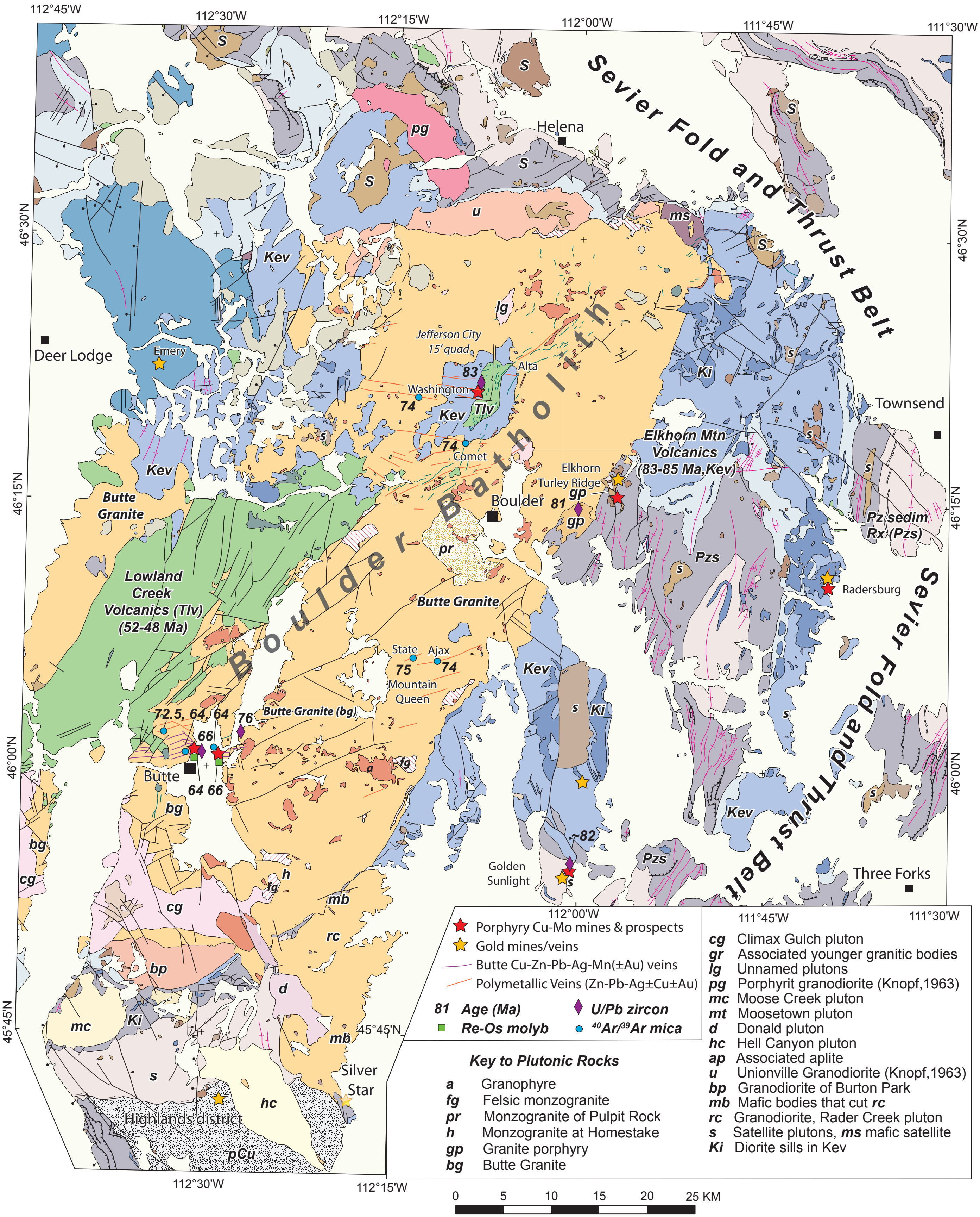

Figure 1. Geologic map of the Boulder Batholith and surrounding areas, modified from Smedes and others (1988). Age data on principal geologic rock units and mineral deposits are from Lund and others (2002, 2007, 2018), du Bray and others (2012), Olson and others (2016, 2017), and references listed therein.

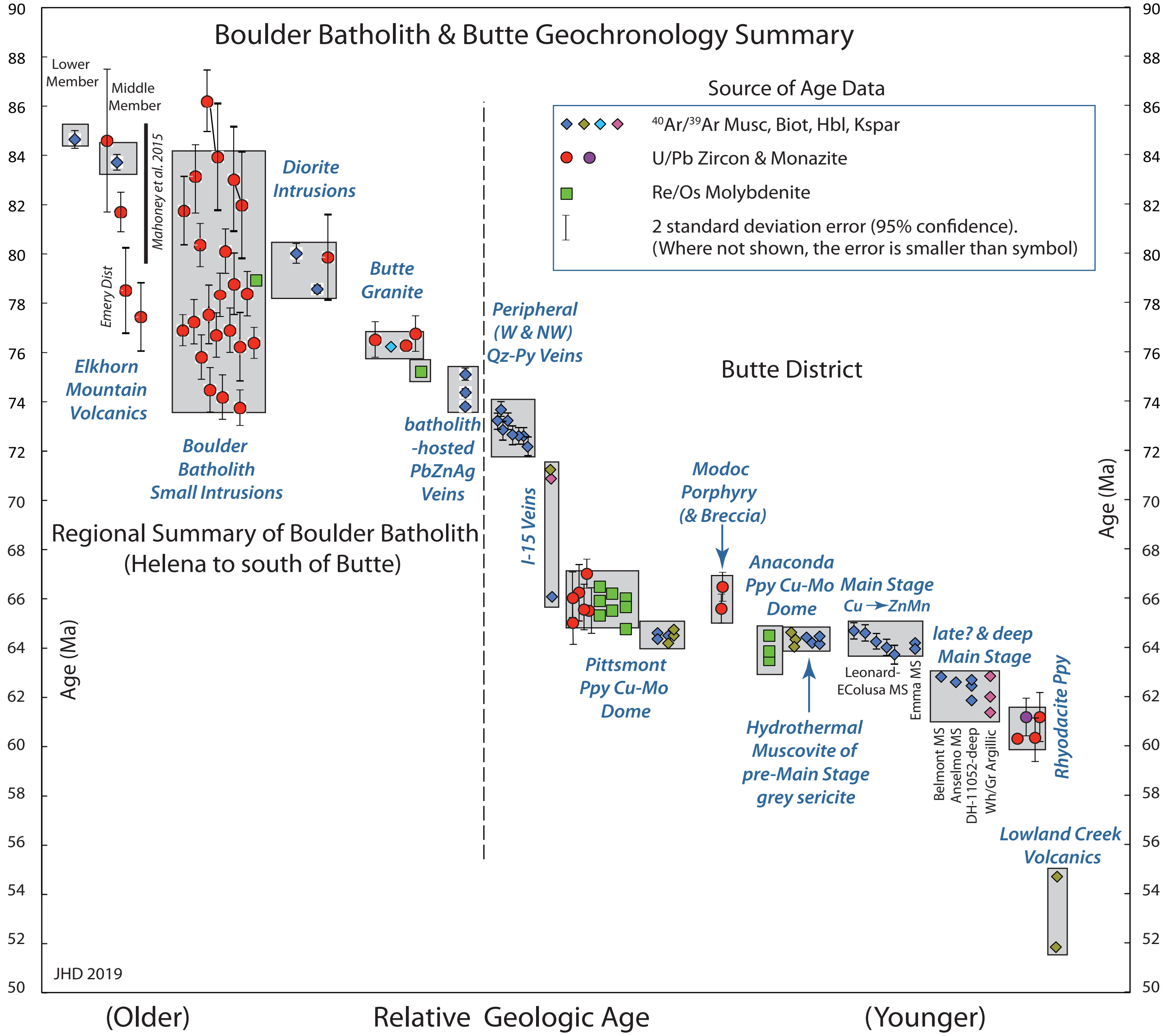

Figure 2. Summary of isotopic ages and geochronology of the Boulder Batholith and Butte District that displays the most reliable age data. Sources of ages include publications of Lund and others (2002, 2018), duBray and others (2012), partial data from Martin and others (1999), Snee and others (1999), Dilles and others (2004, 2006), Houston and Dilles (2013a), Mahoney and others (2015), Olson and others (2016, 2017), and unpublished data including Re-Os ages (H. Stein, written commun., 2004), U-Pb zircon ages (J.H. Dilles, 2000–2107), and 40Ar/39Ar ages (L. Snee, written commun., 2016).

Tectonic Elements

The Boulder Batholith invaded crust with a complex history that contains Archean and Paleoproterozoic Terranes of the Trans-Montana or Big Sky Orogen, including a 1.9–1.8 Ga Paleoproterozoic magmatic arc (Mueller and others, 2002) lying within the northeast–southwest-oriented Great Falls tectonic zone (O'Neill and Lopez, 1985). At about 1.35 Ga, these rocks were rifted and thinned along a west–northwest-oriented aulacogen into which several kilometers of marine to supratidal clastic and carbonate sedimentary rocks of the Belt Supergroup were deposited. Stratabound Cu-Ag-Zn-Pb sulfide ores are widespread in the Belt Basin and could have contributed metals, as well as sulfur, to younger ore deposits. The Boulder Batholith intruded the eastern or Helena salient of the Belt Basin and the overlying thin sequences of late Proterozoic to Jurassic continental margin marine carbonate and clastic rocks.

Late Cretaceous subduction-related magmatism was apparently a result of eastward migration of magmatism that accompanied flattening of the dip angle of the subducting Farallon plate (Lageson and others, 2001; Sears, 2001; English and others, 2003). The flattening increased coupling of the slab with the overlying continental crust, which was shortened by folding and thrust-faulting from about 85 to 65 Ma (Lageson and others, 2001). The Elkhorn Mountain Volcanics were themselves shortened, and the Butte Granite is inferred to have been emplaced into active thrust faults (Kalakay and others, 2001). Hornblende barometry of the Butte Granite in and east of the Butte District provides estimated emplacement depths of 7–9 km for current exposures (fig. 3; Houston and Dilles, 2013a; J. Dilles, unpublished data). The Butte ore deposits formed during a period of uplift and exhumation from 66 to 60 Ma that may have been driven by the last stages of Cretaceous shortening (Houston and Dilles, 2013a).

Coinciding with the eruption of the Lowland Creek Volcanics, detachment-core complex formation, normal faulting, and extension began throughout southwestern Montana and continues today (Foster and others, 2010). The beginning of Eocene extension and magmatism was likely caused by foundering or tearing of the subducting Late Cretaceous flat slab (Christiansen and Yeats, 1992; English and others, 2003). The Boulder Batholith and Butte District lie in the upper plate of the gently east-dipping Anaconda detachment fault, and prior to faulting, lay farther west and close to the Anaconda Core Complex (Foster and others, 2010).

Latest Cretaceous shortening and Cenozoic normal faulting have deformed the Butte District after mineralization. Both paleomagnetic data (fig. 3; Geissman and others, 1980a,b) and the orientations of sheeted aplite sills and porphyry Cu-Mo veins (Houston and Dilles, 2013a) indicate the central part of the Butte District is relatively upright (tilted 5–10° north), in agreement with paleomagnetic data (Geissman and others, 1980a,b), but that exposures on the west and north margins of the district have been tilted ~25–50° northwest by Eocene normal faults (Proffett, 1973, 1979; Proffett and Burns, 1999). A few northeast-striking Eocene faults normally offset ores a small amount; these include the Milwaukee fault (200–400 m), the Middle fault (30 m), and the Rarus fault (105 m; Houston and Dilles, 2013a,b). The most recent offsets are along the Miocene to Recent Rocker, East Ridge, Klepper, and Continental faults. The Continental fault cuts the Continental–Pittsmont porphyry Cu-Mo deposit and relatively displaces the western Pittsmont body ~1,300 m down to the west (Reed, 1979). The Continental mine lies in a horst bounded by the Continental and Klepper faults and contains the deepest exposures in the district.

BUTTE GEOLOGIC STUDIES

In a landmark paper published in 1914, Reno Sales laid out the complex structural pattern of the Butte Main Stage veins, such as the famous Leonard horsetails, and described the zoning of metals from copper outward to zinc, lead, manganese, and silver (Sales, 1914). The geologic story portrayed in Sales' maps was groundbreaking for its detail and accuracy, which served the needs of mine planning and exploration, but was of particular value in litigation arising from Apex Law whereby claims to veins on the surface allowed mining to depth along the veins (Cathro, 2009). Several key apex legal precedents arose from the resolution of Butte mining claim litigation and some cases of underground warfare over conflicting claims by two different mining companies to a single underground vein (Sales, 1964; Malone, 1981; Parry, 2004).

In pioneering studies of altered wall rocks along the margins of the Butte Main Stage veins, Charles Meyer demonstrated that diffusion of aqueous hydrogen ion and sulfur into wall rock and counterdiffusion of calcium and sodium were fundamental to forming the zoned sericite and clay hydrothermal alteration that bordered the veins (Sales and Meyer, 1948). Meyer's fundamental work took advantage of Butte's homogeneous host granite, which enabled meaningful comparison of alteration mineral assemblages at scales spanning centimeters to kilometers, and established Butte as a premier setting for alteration studies (e.g., Meyer and Hemley, 1967). In subsequent work, Meyer (1965) described porphyry–copper-style potassic alteration along the EDM (early dark micaceous alteration, i.e., biotite-rich) veins and selvages, refined and updated the Main Stage metal zoning pattern (fig. 4), and outlined a large low-grade molybdenum zone on the basis of molybdenite occurrences noted over a period of decades in mine map notes and drill core (Meyer and others, 1968).

Subsequent district-scale and regional studies, which were summarized in the 1973 Butte field meeting, included geologic mapping of hypogene and supergene ores in the Butte Berkeley Pit (Miller, 1973; Thompson, 1973), and USGS studies of the

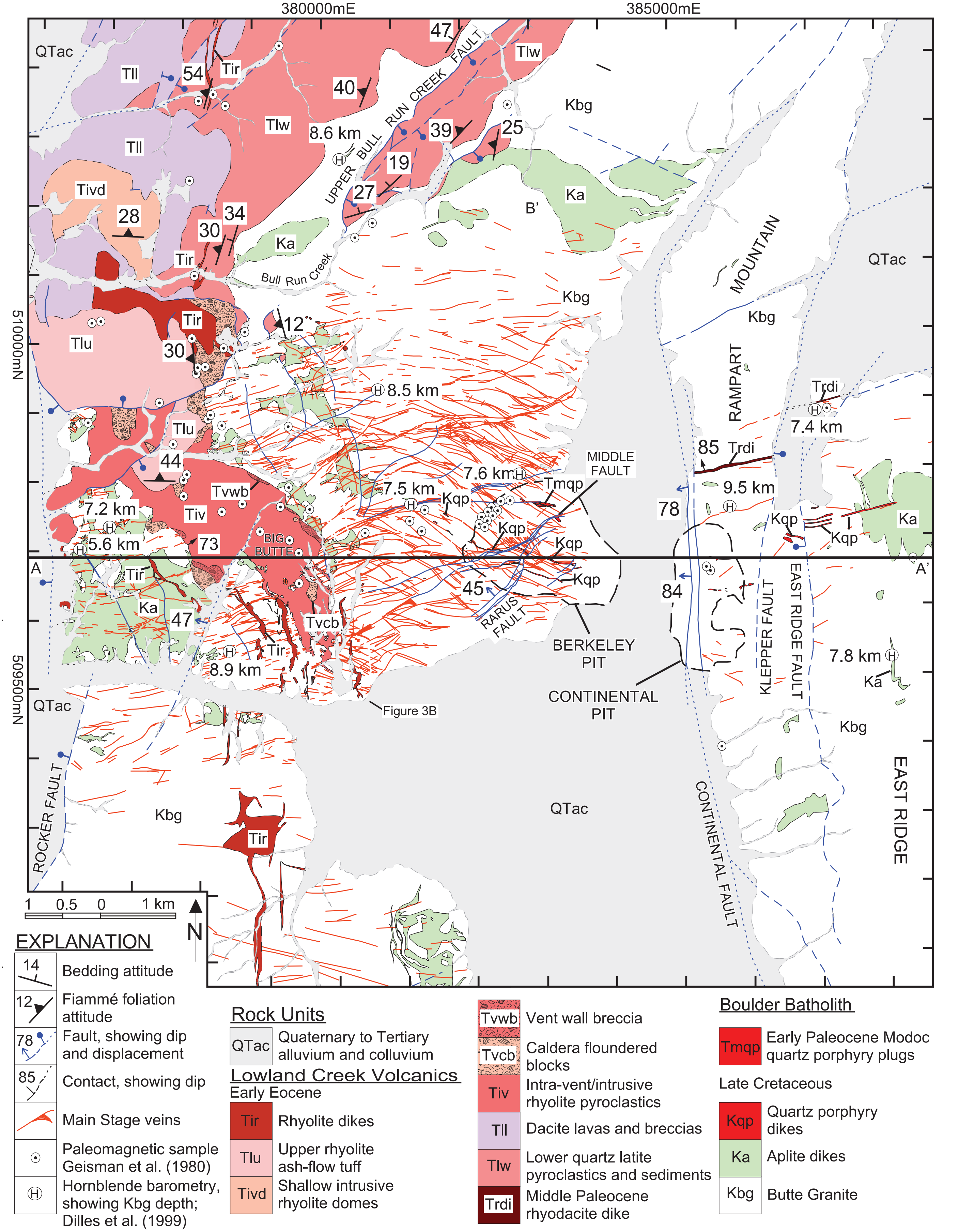

Figure 3. Geologic map of the Butte District, from Houston and Dilles (2013a), with line of cross section A–A' (fig. 15).

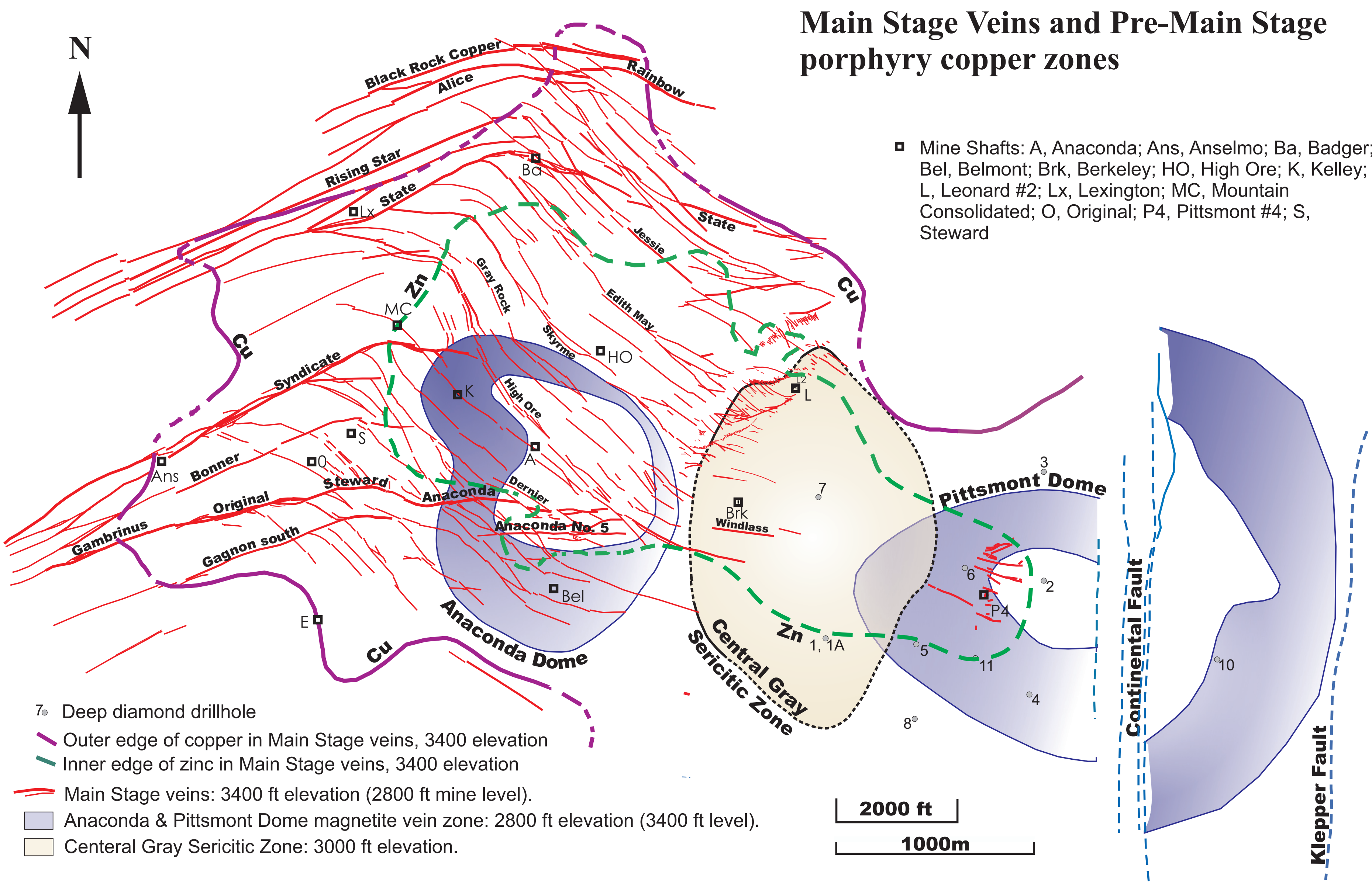

Figure 4. Main Stage Veins (Meyer and others, 1968) superimposed on Anaconda and Pittsmont magnetite veins zones (3400 level; 2800' elevation) and the central gray sericite zone (3000' elevation). Main Stage vein Cu and Zn zone boundaries from Meyer and others (1968), with addition to the innermost Zn boundary (2800 level) based on deep surface drillholes in the eastern region.

field geology, petrology, and geochemical composition of the regional rock units including the pre-mineral late Cretaceous Elkhorn Mountains Volcanics and Boulder Batholith as well as the post-mineral Eocene Lowland Creek Volcanics (Smedes, 1962; Smedes and others, 1973, 1988; Tilling, 1973, 1974). In addition, John Proffett (assisted by G. Burns) produced the first modern geologic map of the Butte District and updated the structural geology (Proffett, 1973; Proffett and Burns, 1999; Proffett and others, 1982). These studies documented the nature and amount of strike-slip and normal offset on the Main Stage veins, as well as post-mineral faults that offset and rotate the Lowland Creek Volcanics to produce moderate west–northwest dips. Proffett's hypothesis of post-mineral tilting led to paleomagnetic studies by John Geissman, who concluded that the Butte Granite ore host within the district is tilted only ~5–10° to the north (Geissman and others, 1980a,b).

The EDM assemblage as described by Meyer (1965) from the deep western mines (e.g., Steward) is characterized by replacement of primary granite minerals by biotite, muscovite, alkali feldspar, and quartz with lesser chlorite, anhydrite, calcium-bearing sidero-magnesite, magnetite, hematite, pyrite, and chalcopyrite. Meyer called the EDM and quartz–molybdenite veinlets "pre-Main Stage," and pointed out their similarities to recognized characteristics of veinlets of porphyry copper–molybdenum deposits (Meyer, 1965*)*. In succeeding studies of the EDM veins, George Brimhall (1973, 1977) applied alkali feldspar equilibrium to estimate potassic alteration temperatures that exceed 600°C. In overlapping studies, Steve Roberts (1973, 1975) estimated potassic alteration temperatures exceeding 600**°**C on the basis of andalusite–muscovite–feldspar–quartz equilibrium. Roberts also described and measured properties of fluid inclusions in Butte potassic alteration, where he found surprisingly dense fluids indicating trapping pressures of about 2.5 kb, placing the Butte magmatic-hydrothermal system at a depth exceeding 7 km—more than twice the depths estimated for most other porphyry copper deposits (cf., Sillitoe, 1973, 2010; Seedorff and others, 2005).

The three-dimensional surface defined by Meyer and others (1968), informally called the "moly dome," was the first district-scale feature to define the shape of what later became recognized as the Butte porphyry copper deposit, but its circular closure at shallow depth on its eastern front seemed contradictory to the independently recognized stockwork EDM and quartz–molybdenite veining in the footwall of the Continental fault, 3 km to the east. Furthermore, Roberts (1973) defined and plotted an east–west elongated zone of hydrothermal biotite replacement of hornblende that included the Meyer moly dome on the west and the Continental EDM veinlets on the east. Brimhall (1977) defined a similar east–west elongated molybdenite vein zone.

In the middle 1970s, Anaconda geologists Brimhall, Roberts, John Proffett, and George Burns mapped crosscuts and drill core on the Kelley 2000-ft and Steward 3400-ft mine levels. That effort continued into the late 1970s by Reed, leading to the recognition of a dome-shaped zone of magnetite veins, which, coupled with molybdenum assays, showed that the Meyer moly dome coincides with a distinctly separate porphyry copper center that closes off in the western region (Reed, 1979, 1980, 1981). Subsequent deep drilling (1978+) from the surface in the center and eastern parts of the district confirmed that the Butte porphyry copper deposit consists of two separate porphyry copper bodies (Reed, 1979), the Anaconda dome in the west and the Pittsmont dome in the east (figs. 5, 6). The term "dome" follows Meyer's informal usage, but it is significant for its definition of domical bodies as opposed to vertical cylindrical bodies characteristic of porphyry copper deposits formed at shallower depths (e.g., Seedorff and others, 2005).

The Butte deep drilling project extended into the early 1980s. The drillholes extended to a maximum length of 7,500 ft (2.3 km), deeply exploring more than half of the volume of the district that was largely unknown before. The deepest holes traversed completely through the newly recognized Pittsmont porphyry copper body, revealing for the first time that the mineralized vein stockwork transitions at depth into a massive barren quartz stockwork, overprinted on its western side by intense sericite–quartz–pyrite alteration (gray sericitic, GS; Reed, 1979). The first deep hole (DH #1 and 1A wedge-off) intersected gray sericitic alteration in the center of the district that led to recognition of a large elliptical body of pervasive sericite–quartz–pyrite alteration in the center of the district that predated and largely controlled the Main Stage fracture configuration, including the Butte horsetail ores, and the distribution of Butte advanced argillic alteration (Reed 1979, 1981).

A collaborative research project initiated by the

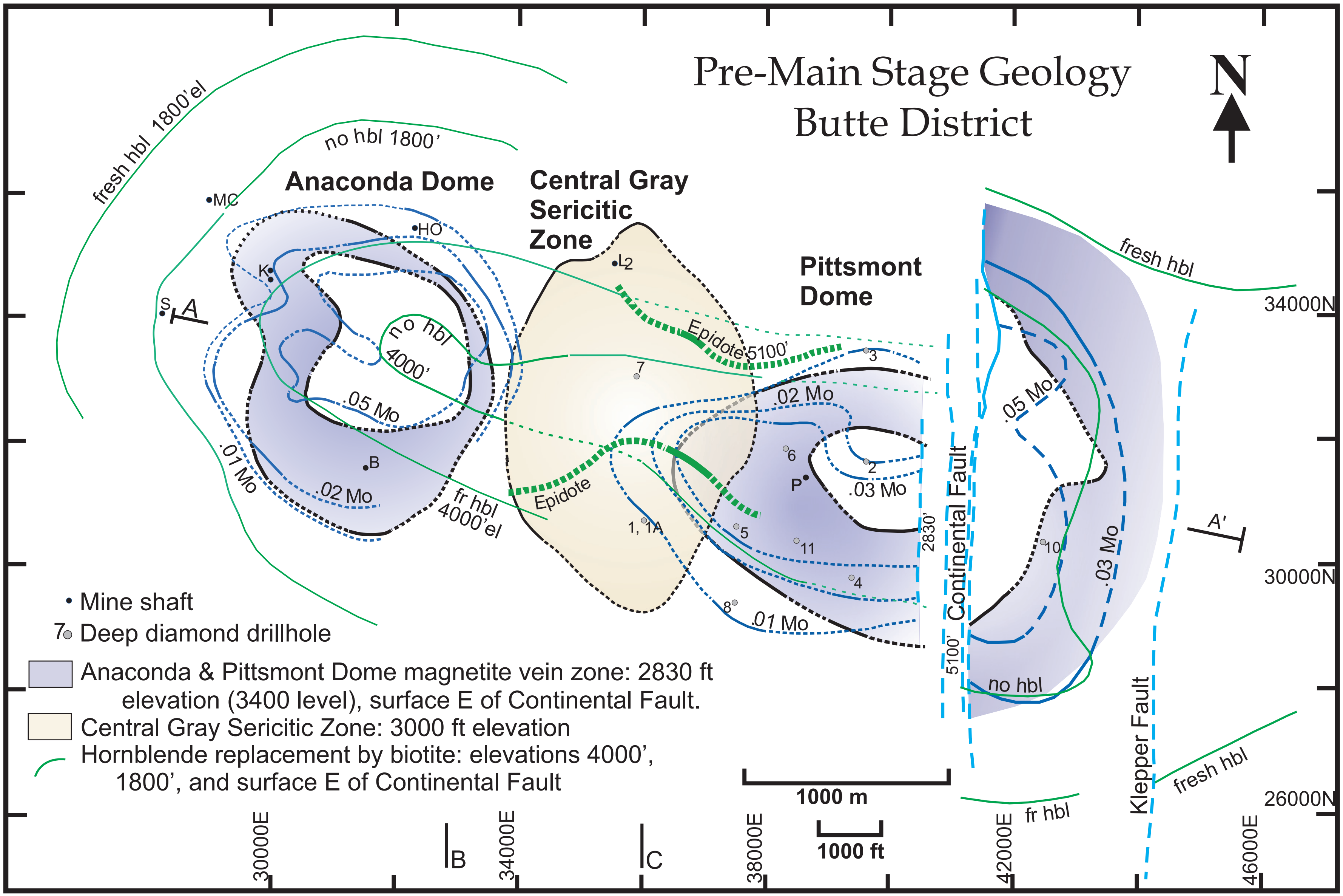

Figure 5. Butte District porphyry-copper stage geology, showing features as follows (elevation in feet): Anaconda and Pittsmont domes defined by magnetite vein zones (2830', surface in east), central gray sericitic zone (3000'), molybdenum grade (2830', surface in east), above from Reed (1979–1981); epidote alteration in central region (5100' el) from Page (1979) with eastward extensions by Reed (1981); hydrothermal biotite replacement of granite hornblende (1800', 4000', surface) from Roberts (1973) in Anaconda dome and immediately east of Continental fault, and from Dilles in Pittsmont dome and east of Klepper fault. One trace of the Continental fault is shown at 2830' elevation, and others at 5100' elevation. The Klepper fault is shown at the surface. The East Ridge fault (fig. 3; not shown here) occurs just east of the edge of biotite contours. The location of east–west cross section (fig. 6) is marked A–A'. Line segments B and C mark cross sections of figures 9 and 11.

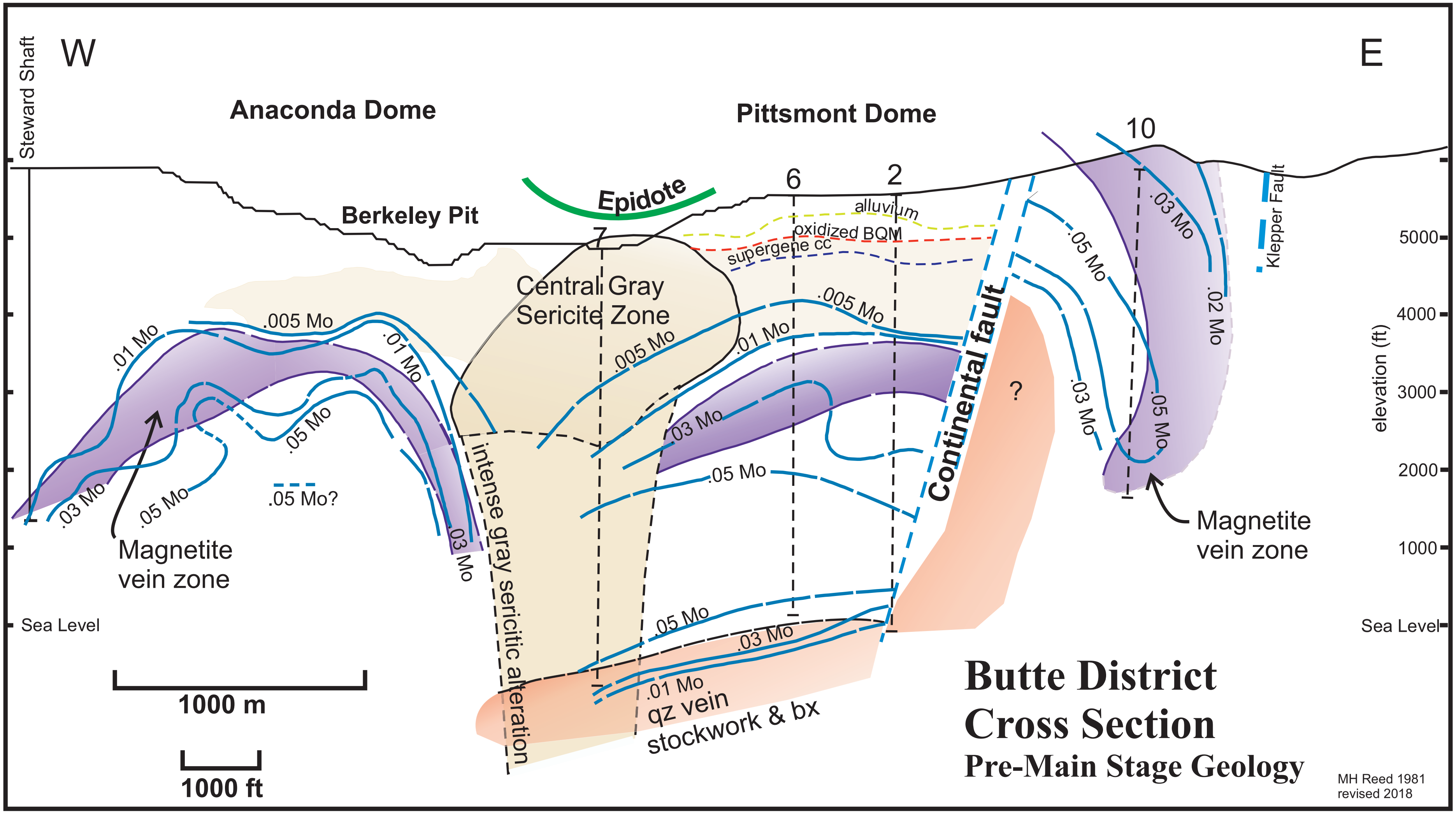

Figure 6. East–west geologic cross section through the Butte porphyry copper–molybdenum deposit along A–A' of figure 5 (Reed, 1979). The main mineral centers are the Anaconda dome in the west and the Pittsmont dome in the east. Each of these is defined by a magnetite vein zone (purple) and by molybdenum grade contours (blue lines), and both have overlying sparse GS veining (light yellow-tan). Between the two domes lies a bulb-shaped body of intense gray sericite–quartz–pyrite alteration (GS). The deepest drilling intersected a mixed granite and quartz porphyry breccia mingled with intense stockwork quartz veins and breccia of quartz veins beneath the center of the mineralized system, including the bottom of DH 2 beneath the Continental fault.

University of Oregon and Oregon State University, beginning in 1996, was funded by the National Science Foundation and involved researchers from the U.S. Geological Survey and close cooperation from Montana Resources, the owner of the producing Butte mine. The new research project relied significantly on core from the 1978–1983 deep drilling project as well as core and crosscut samples from the western mines, which provided samples for studies of pre-Main Stage veins and alteration using fluid inclusions and quartz SEM-cathodoluminescence (e.g., Rusk and Reed, 2002; Rusk and others, 2004, 2008a,b), oxygen and hydrogen isotopes of alteration minerals (Zhang, 2000), sulfur isotopes (Field and others, 2005), studies of titanium diffusion and geothermometry in alteration and vein minerals (Mercer and Reed, 2013; Mercer and others, 2015), and an examination of quartz vein formation processes, including those in the deep barren quartz vein stockwork (e.g., Acosta and others, 2017, 2018, 2019). Recent geochemical modeling shows how reaction of the Butte Granite with a single magmatic fluid composition accounts for the wide range of pre-Main Stage alteration assemblages (Reed and others, 2013).

During this period and continuing to the present, numerous geochronology studies have refined our understanding of Butte geologic history. Studies include the following: Lawrence Snee's $^{40}Ar/^{39}Ar$ ages of igneous and hydrothermal micas (Snee and others, 1999); U-Pb zircon TIMS ages of intrusions (Martin and others, 1999; Martin and Dilles, 2000); and Re-Os ages of molybdenite by Holly Stein (Dilles and others, 2004). Parallel studies by the USGS that include $^{40}Ar/^{39}Ar$ ages of hydrothermal micas and U-Pb Shrimp-RG ages of zircon from intrusions of the Boulder Batholith and Butte District are reported in Lund and others (2002, 2018) and du Bray and others (2012). Additional U-Pb zircon ages have been obtained for Butte District zircons by Shrimp-RG (Dilles and others, 2004, 2006, and unpublished data).

Previously unreported work from the deep drilling and related work (Reed, 1979–1981) plus details of the various recent studies make up the content of this chapter, which pulls together Butte studies since the review by Meyer and others (1968) and the 1973 Butte field meeting (e.g., Roberts, 1973; Brimhall, 1973). The latter was followed by additional works by Brimhall (1977, 1978, 1979) and Brimhall and Ghiorso (1983).

In the early 1980s the Butte District and the nearby Anaconda smelter sites were declared Environmental Protection Agency superfund sites owing to acidic mine drainage and heavy metal contamination of streams and groundwater. The fundamental problem in Butte is the chemical breakdown and physical erosion of mine waste rock and mill tailings dumped on the surface since the late 1800s. In addition to being a world-class ore deposit, the Butte mining legacy has made Butte a world-class example of serious heavy metal pollution. Since the EPA Superfund site declaration, ARCO and the EPA have endeavored to mitigate the environmental damage through an extensive series of innovative measures for controlling runoff, trapping heavy metals, minimizing sulfide mineral oxidation, and processing of runoff waters to extract heavy metals. These measures are explored in detail in another chapter of this volume (Gammons and Duaime, 2020).

ROCKS OF THE DISTRICT

Butte Granite, Aplites

The Butte intrusion is composed largely of granite in the IUGS classification (Lund and others, 2002), but was formerly called a quartz monzonite (Emmons and Tower, 1897; Weed, 1897, 1912). In the Butte District, the granite is medium-grained and composed of subequal amounts of quartz, plagioclase (mostly $An_{40–48}$), and K-feldspar (generally 5–10 mm, and locally up to 30 mm length) as well as about 20 vol% biotite and hornblende, plus accessory magnetite, ilmenite, titanite, apatite, and zircon (Meyer and others, 1968; Roberts, 1973). In the Butte District, the granite is relatively homogeneous, excepting aplites, but USGS workers have described several textural variants with slightly different mineral proportions in the widespread exposures in the Boulder Batholith (Tilling, 1964; Smedes, 1966; Smedes and others, 1988). Across the batholith the composition of the Butte Granite ranges widely from 60 to 73 wt% SiO_2 (du Bray and others, 2012), but in the Butte District generally has 64 wt% SiO_2. Martin and others (1999) reported a U/Pb TIMS zircon age of 76.3 ± 0.2 Ma based on a TIMS analysis of a sample from the Butte District, whereas U/Pb zircon analyses by Shrimp-RG provide ages of about 76.5 ± 0.7 Ma and 76.8 ± 0.8 Ma (fig. 2; du Bray and others, 2012).

Within the Butte District, the granite is cut by several types of leucocratic sill-like intrusions with 74–76 wt% SiO_2. West of Big Butte several sheets exceed 10 m in thickness and have been described as granoaplite (Meyer and others, 1968). The bodies range from fine- to medium-grained (0.5–3 mm) and are dominated by quartz and K-feldspar with seriate texture, minor sodic plagioclase, and 2–5 vol.% biotite. Elsewhere throughout the district, there are ~0.5- to 3-m-thick aplite–pegmatite sill-like bodies that consist dominantly of 1 mm sugary textured quartz and K-feldspar accompanied by 1–2 vol.% biotite (Houston and Dilles, 2013a). The centers of thick aplite dikes locally contain pegmatites with cavities lined with smoky quartz, biotite, tourmaline, muscovite, and sparse sulfides including pyrite, chalcopyrite, and rare molybdenite. The granoaplite, aplite, and pegmatite bodies are inferred to be the same age as the host Butte Granite based on limited isotopic ages (Lund and others, 2002; H. Stein, unpublished data).

Porphyry Intrusions

Several porphyry dikes and plugs are recognized in the Butte District, of which two types are syn-mineral "quartz porphyry" and one is a post-mineral "rhyolite." Three occurrences of quartz porphyry dikes are biotite rhyolite of similar composition and mineralogy, and average about 70 wt% SiO_2. The post-mineral rhyolite is a biotite rhyodacite porphyry and averages 67–71 wt% SiO_2, and is hereunder identified as "rhyodacite" following the usage of Houston and Dilles (2013a,b) and distinguishing it from the syn-mineral quartz porphyries and post-mineral rhyolite dikes associated with the Lowland Creek Volcanics.

In the Pittsmont porphyry Cu-Mo center, quartz porphyry forms two parallel dikes about 100 m apart and 5–10 m in width that strike N85°E and dip ~80–85°S. The dikes can be traced on the surface from the Continental Pit to the east of I-15, and to the west in the Pittsmont dome in the subsurface. The dikes contain about 40–50 vol.% percent phenocrysts comprising sodic plagioclase, rounded quartz (~5 vol.%), and biotite (2–5 vol.%, commonly partly altered to muscovite), which are set in an aplitic groundmass. On the basis of Ti-in-quartz geothermometry and experimental phase petrology (Naney, 1983; Mercer and Reed, 2013), the phenocryst assemblage is consistent with emplacement at about 700°C. The age (fig. 2) of the Pittsmont porphyry dikes and related porphyry Cu-Mo ores is about 66 Ma based on zircon U/Pb ages of 67 ± 1 Ma (Lund and others, 2002), 65–66 Ma (Lund and others, 2018) and 66–67 Ma (Dilles and others, 2006), and Re-Os ages of hydrothermal molybdenite (65.5–66 Ma; Dilles and others, 2004).

The Steward dikes are petrographically similar to the Pittsmont dikes and form a second set of parallel quartz porphyry dikes that strike ~N70°W and dip ~80–85°S. The dikes are central to the western Anaconda porphyry Cu-Mo center. Geochronology on these dikes and related ores remains uncertain (fig. 2). Lund and others (2018) obtained a U/Pb zircon age of 66.3 ± 1.3 Ma for a Steward dike, but this is not a robust age; the 12 individual zircons used to calculate the mean range from 64 Ma (n = 3) to 70 Ma (n = 2). Possibly, the Steward dikes are younger and about 64 Ma, which is the age of mineralization on the basis of three Re-Os ages of molybdenite (63.4, 63.9, and 64.5 Ma, all ±0.2 error) from the Anaconda center (Dilles and others, 2004).

The quartz porphyry dikes in the Pittsmont and Anaconda domes are centered within porphyry Cu-Mo mineralization, as further examined below. For example, hydrothermal biotite breccias (fig. 7) occur in dike walls where they co-intruded with the dikes and incorporated fragments of quartz porphyry and Butte Granite. Some granite fragments contain cut-off veins (fig. 7C). Quartz porphyry dikes cut and are cut by early EDM porphyry copper veins. Drill core and underground mine biotite breccia intercepts occur from ~5,000 ft (1,500 m) elevation to below 1,500 ft (450 m) elevation, and the breccias' uppermost occurrences coincide with the upper limits of quartz porphyry dikes on the district scale.

Mineralogically and texturally similar quartz porphyry fragments occur together with clasts of Butte Granite and aplite in the plug-like and 100-m-diameter body of Modoc breccia exposed on the north wall of the Berkeley Pit (Thompson, 1973; Minervini, 1975; Houston and Dilles, 2013a). Whereas the Pittsmont and Steward dikes are cut by quartz–molybdenite, quartz–chalcopyrite–pyrite, and biotite-bearing veins, the quartz porphyry in the Modoc breccia lacks these veins and rather is altered to assemblages with chlorite, sericite, and pyrite with relict partly altered igneous plagioclase. Clasts of Butte Granite are cut by quartz–molybdenite veins that do not cut the breccia matrix, and therefore the Modoc breccia postdates Mo mineralization. A Shrimp-RG U/Pb zircon age of 66–66.5 Ma for porphyry dike fragments is similar to the age of porphyry dikes in the Pittsmont Cu-Mo center (fig. 2; J.H. Dilles, unpublished data).

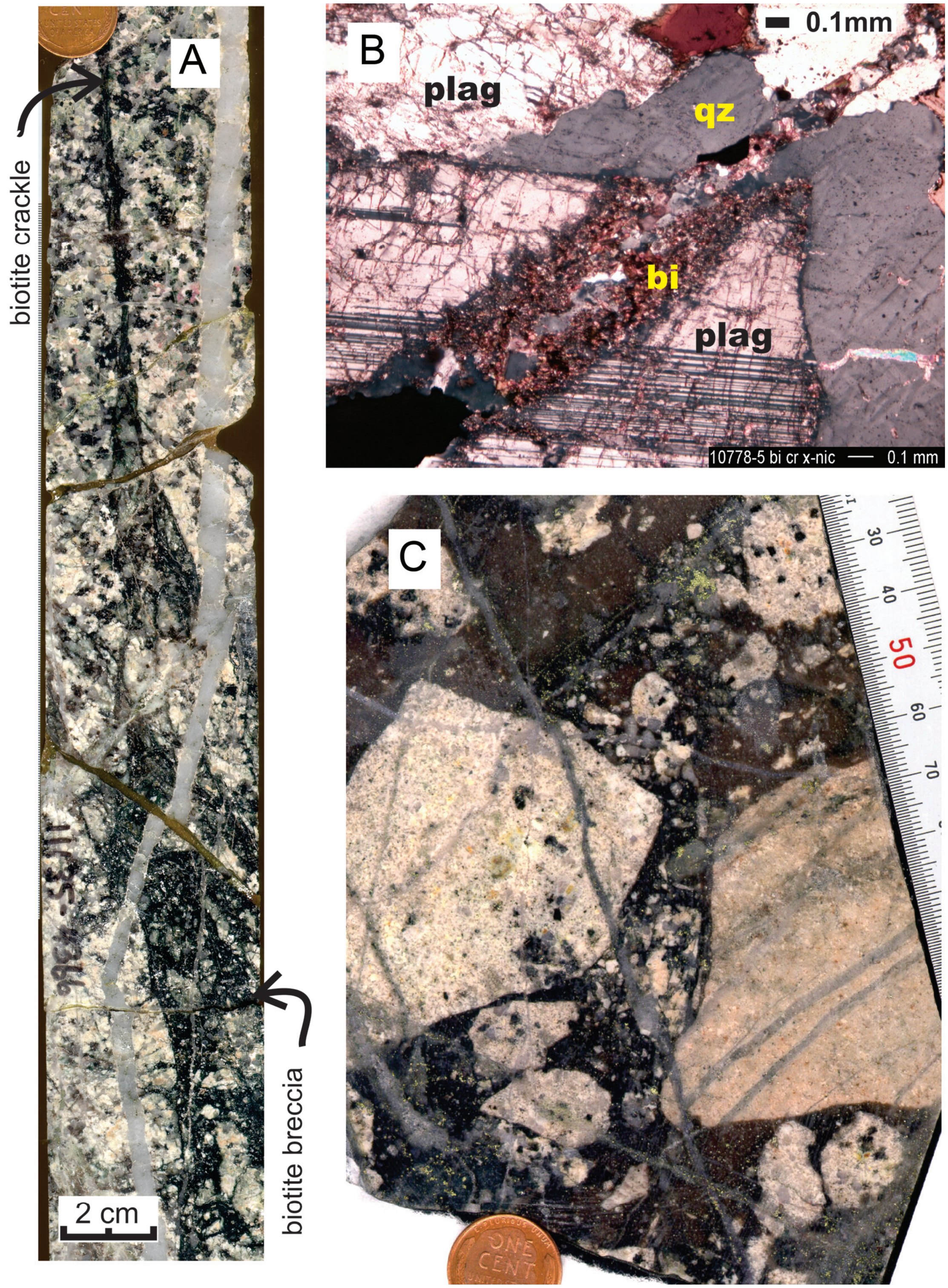

Figure 7. (A) Biotite breccia bleeding upward into biotite crackle veinlets, cut by 4- to 8-mm barren quartz veinlet (11135-4366, deep in center of Pittsmont dome). (B) Photomicrograph (x-polars) of biotite crackle cutting plagioclase and quartz of the Butte Granite. The quartz-rich center of the crackle is bordered by shreddy biotite where it cuts plagioclase, but not quartz (Kelly 3400 level, 10778-5). (C) Biotite breccia with fragments of aplite and granoaplite, some with quartz veins truncated at the fragment margin. Other veins cut the breccia (Continental Pit, Bu96mr-13).

The youngest dike is a rhyodacite porphyry, referred to as “rhyolite” by Meyer and others (1968). This east–west-striking dike is ~30 m wide north of the Continental Pit, and was traced in the underground mine workings westward from the Leonard mine west to the Anselmo mine. The rhyodacite contains about 60 vol.% <0.05 mm groundmass and phenocrysts of 0.3–3 mm sodic plagioclase (15–18 vol.%) and quartz (10–12 vol.%), 0.5 mm biotite (5 vol.%), and 2–20 mm K-feldspar (2–7 vol.%). The rhyodacite dikes cut the Main Stage veins, and are weakly to strongly hydrothermally altered with partial replacement of plagioclase by kaolinite, smectite clays and calcite, and up to 1 vol.% pyrite. U/Pb ages of zircon and monazite indicate an age of about 60–61 Ma (Houston and Dilles, 2013a; Lund and others, 2018; J.H. Dilles, unpublished data).

VEINS AND ALTERATION IN THE BUTTE PORPHYRY COPPER DEPOSIT

The form of the Butte porphyry copper deposit is defined by the distribution of magnetite-bearing veins, quartz–molybdenite veins, and hydrothermal alteration spanning from the deep potassic (EDM) to peripheral sericitic and propylitic zones. Butte alteration and veins are classified by conspicuous distinguishing features such as vein mineral content, alteration envelope assemblages, and structural style. Following in the tradition established with the term "EDM" (early dark micaceous, Meyer, 1965), which refers to a biotite-rich alteration assemblage and to veins bordered by that alteration, we refer similarly to additional alteration types designated PGS (pale green sericitic), DGS (dark green sericitic), and GS (gray sericitic). These alteration types were defined (Reed, 1979) based on observations in drillcore and crosscuts mostly on the Steward 3400 mine level and the Kelley 2000 and 3400 levels, including diamond drillholes that extended well below the 3400 level.

The veins of the potassic series, EDM, PGS/EDM, PGS/DGS, DGS, GS/DGS, and propylitic zone (PRP), are defined by their alteration envelopes and are the oldest of the Butte Pre-Main Stage veins. (The slashes in the preceding list indicate inner and outer zones of paired envelopes on single veins.) They are contemporaneous as a group, and all contain alteration K-feldspar. The potassic series veins are cut by quartz–molybdenite and barren quartz veins, which mostly lack alteration and are distinguished by vein minerals. Quartz–molybdenite veins are cut by a late set of pyrite–quartz veins with GS alteration (see below) and by the late, fissure-filling veins of the Main Stage (Meyer and others, 1968). The alteration terms, such as EDM, PGS, DGS, and GS are petrologic rock names referring to specific mineral assemblages that form envelopes on veins, as laid out in table 2. (The term "sericite" refers to hydrothermal white mica of muscovite composition.)

Butte Mineral Zones, Veinlets, and Alteration in the Anaconda and Pittsmont Domes

The Butte porphyry copper-style mineralization is defined by the Anaconda and Pittsmont domes that are each 2 km in diameter (fig. 5) aligned along a swarm of quartz porphyry dikes. Between the two domes is a third 1.2 x 1.8-km zone of intense pyrite–quartz veins with a pervasive sericite–pyrite–quartz alteration. The Anaconda and Pittsmont domes consist of overlapping concentric shells of millimeter- to centimeter-scale stockwork veinlets of the potassic series, all with alteration envelopes that are used to distinguish the vein types. The potassic series veins gradationally change upward and outward over a radial span of about 1 km, as shown in table 3.

Alteration envelopes on veins of the potassic series, including the gray sericitic (GS), characteristically include added potassium on an absolute volume basis. All contain sericite (muscovite), and all but GS contain newly formed K-feldspar. The deepest contain biotite and distinctive andalusite, giving way upward to chlorite-bearing assemblages, then shallow chlorite plus epidote in the propylitic assemblage.

Early Dark Micaceous (EDM), Biotite Crackles, and Biotite Breccia

The deepest veins of the potassic series are quartz–chalcopyrite–pyrite veins with biotite–K-feldspar–sericite ± andalusite alteration (fig. 8A) that Meyer (1965) designated "EDM," and Roberts (1975) and Brimhall (1977) further described. The earliest Butte veinlets are a variant of EDM called "biotite crackles," consisting of millimeter-width biotite-altered wall rock along microscopic quartz veins (figs. 7A, 7B). Some biotite crackles emanate directly from biotite breccias (fig. 7A), which occur prominently at the apices of quartz porphyry dikes, and in dike walls, where the porphyry has intruded its own apical breccia. Biotite breccia consists of sand-sized to centimeter-scale rotated angular to subrounded fragments of granite and aplite suspended in a dark matrix of biotite, quartz, K-feldspar, chalcopyrite, and pyrite (Brimhall, 1977). The direct physical connection of biotite crackles to biotite breccia, and the breccia to porphyry, indicate that the hydrothermal fluids that formed the EDM potassic mineral assemblage emerged from porphyry magma.

Table 2. Pre-Main Stage alteration types.

Alteration Type; Zone	Defining Minerals and Textures, Alteration Mineral Reactions: [granite mineral] -> alteration mineral	Metallic Minerals in Veins and Alteration
Early dark mica, **EDM**; beneath and lapping into mt vein zone	Brown & green shreddy biotite; kf rims ms [plag] -> ms, kf, shreddy bi, plag: ab(94-98), an(23-30) ± and ± cor, anh, carb [kf] -> ms, kf: or(93), bi [hornb]->bi, anh, kf [bi]-> bi (re-xl, increased Mg/Fe)	cp, py, ± mt mb (veins only)
Pale green sericitic, **PGS**; mt vein zone. PGSk includes kf PGSs lacks kf, chl	Pale green ms, kf & fine chl; granite texture destroyed [plag, kf]->ms ± kf, qz, chl$^-$ (ser island txt) [bi, hornb]-> ms, chl, carb	cp, py, mt
Dark green sericitic, **DGS**; upper mt zone and above.	Dark green chlorite; granite texture intact [plag,]->pale green ms ± kf, qz, chl [kf]-> ms ± kf, qz [bi]-> chl unit pseudomorph, rt grid	cp, py ± mt
Propylitic, **Pr**; peripheral	ep, chl; granite texture intact [plag]->ser, ep, chl, kf$^-$ [kf]->largely fresh [bi]-> chl, py [hornb]->ep, chl, py	sl, gn, cp, py ± rc
Gray sericitic, **GS**; exterior to mt zone; central GS zone	gray qz, ser, pyrite; texture destroyed [plag, kf]->qz, ms, py [bi, hornb]->ms, py, qz, Mg-chl, rt	py, cp$^-$
sericitic with remnant biotite, **SBr**; exterior to mt zone; central GS zone	Texture mostly destroyed [plag, kf]->qz, ms, py [bi]-> remnant bi (increased Mg/Fe), ms, py	py, cp$^-$

Note. Mineral abbreviations: ab, albite; an, anorthite; and, andalusite; anh, anhydrite; bi, biotite; carb, carbonate; chl, chlorite; cor, corundum; cp, chalcopyrite; ep, epidote; gn, galena; hornb, hornblende; kf, K-feldspar; mt, magnetite; ms, muscovite; plag, plagioclase; py, pyrite; mb, molybdenite; qz, quartz; rc, rhodochrosite; rt, rutile; ser, sericite; sl, sphalerite;

Table 3. Spatial distribution of veins of the pre-Main Stage from deepest upward and outward.

Vein Content	Alteration Envelope (1–3 cm width)
Quartz–chalcopyrite–pyrite	Biotite–K-feldspar–sericite (early dark mica, EDM)
Quartz–chalcopyrite–magnetite–pyrite	Zoned: outer biotite-rich envelope (EDM); inner sericite–K-feldspar–chlorite, but lacking biotite (pale green sericitic, PGS)
Quartz–chalcopyrite–pyrite ± magnetite	Zoned: inner PGS; outer abundant chlorite, K-feldspar–sericite (dark green sericitic, DGS); some envelopes DGS-only
Pyrite–quartz	intense sericite–quartz–pyrite (gray sericitic, GS)
Quartz–sphalerite–galena–chalcopyrite–(rhodochrosite)–pyrite	Chlorite, epidote, K-feldspar, sericite (propylitic)

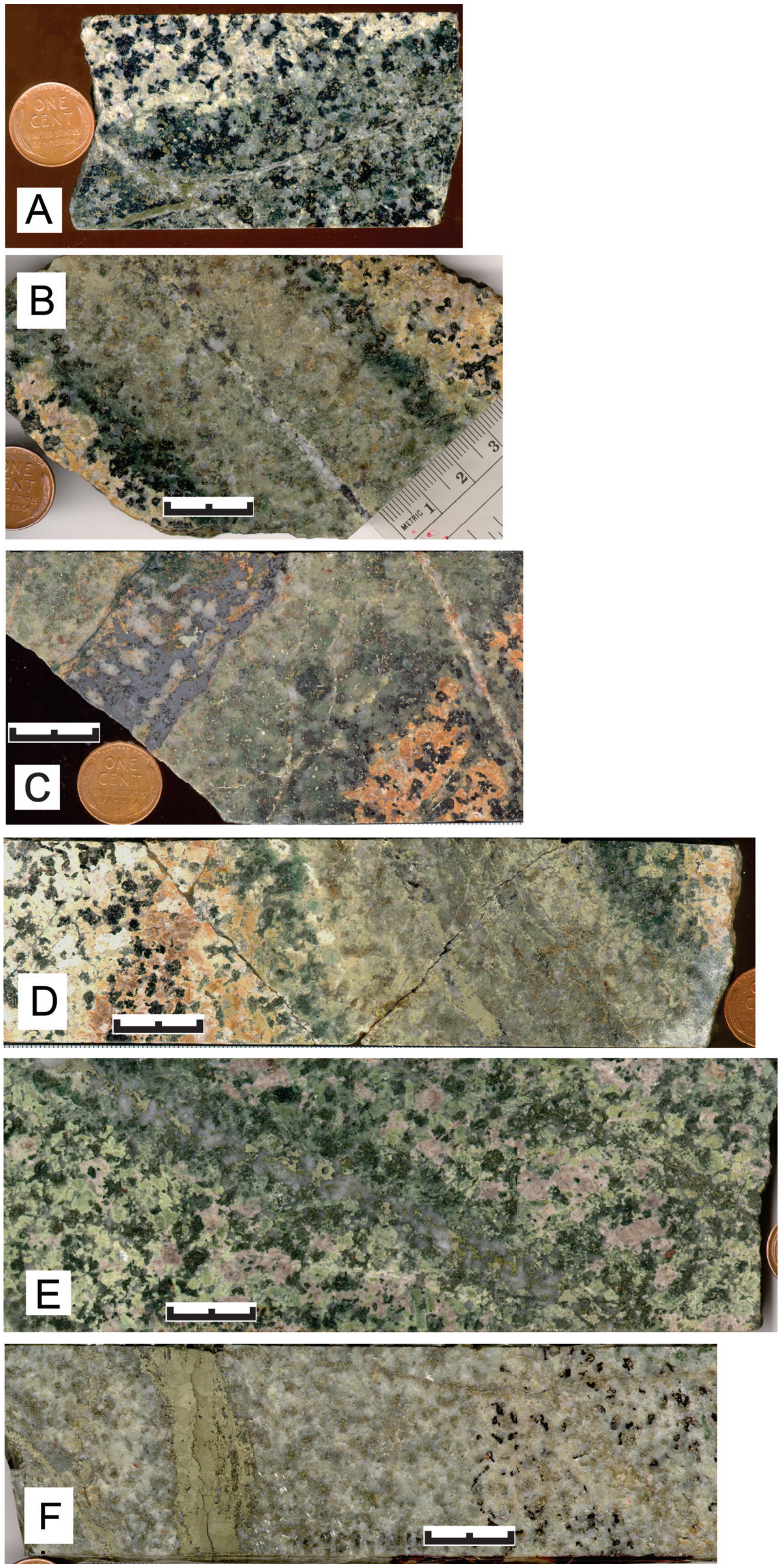

Figure 8. Polished slabs of Butte veins illustrating alteration and vein types. Scale bar is 20 mm; coin is 19 mm in diameter; all images are at the same scale. See table 2 for definitions of alteration terms used in the following descriptions. (A) 2 mm quartz–pyrite–chalcopyrite vein with EDM envelope (deep center of Pittsmont dome 11135-4414). (B) Quartz–pyrite–chalcopyrite–magnetite vein with PGS/EDM alteration, surrounded by later argillic alteration (10778-6, 3400 level of northwest Anaconda dome). (C) 27 mm quartz–magnetite–pyrite–chalcopyrite vein with PGS/EDM envelope, illustrating abundant magnetite that is characteristic of much of the magnetite zones shown in figures 4, 5, 6, and 9 (10961-766, north flank Anaconda dome, 3,200 ft elevation). (D) Pyrite–quartz vein bordered by zoned GS/DGS alteration envelope, surrounded by late argillic alteration (10854-1261, 2000 level, center of Anaconda dome). (E) 8 mm quartz–pyrite–chalcopyrite vein with DGS alteration and an outer envelope of DGS alteration with remnant primary K-feldspar (pink; 10854-27, central Anaconda dome, 2000 level). (F) Pyrite vein with GS/SBr envelope (10969-1410, south flank of central GS zone.

In his petrography and electron microprobe studies, Roberts (1975) described EDM alteration containing fine-grained “shreddy”-textured hydrothermal biotite, accompanied by K-feldspar (Or_{90}), quartz, muscovite, andalusite, albite ($An_{1–6}$), plagioclase ($An_{23–30}$), anhydrite, and corundum. Granite plagioclase is An_{40-48} (Roberts, 1975) and is distinct from the newly precipitated EDM plagioclase and albite, which reflect the peristerite gap in plagioclase solid solutions (Reed and others, 2013). As Roberts pointed out, the equilibrium of andalusite with muscovite, K-feldspar, and quartz indicates a temperature of 600ºC at 2 kb pressure (Sverjensky and others, 1991; Spear, 1993), which matches temperatures determined for EDM and quartz–molybdenite veins by Mercer and Reed (2013) from concentrations of Zr in rutile, Ti in biotite, and Ti in quartz, described below. At shallower depths, EDM alteration lacks andalusite and lacks An_{26}–plagioclase while keeping its distinctive biotite, muscovite, and K-feldspar.

Biotitization of Hornblende

Roberts (1973, 1975) showed that granite hornblende is converted to fine-grained biotite, quartz, and anhydrite in the volume of granite occupied by biotite crackles and EDM veins described above. Within Roberts’ biotitization volume (fig. 5), he also identified a pervasive change in primary biotite composition, added disseminated pyrite and chalcopyrite that partially replace mafic minerals, and conversion of sphene to anhydrite, quartz, and Fe-Ti oxides.

Pale Green Sericitic Alteration (PGS) and the Magnetite Vein Zone

The EDM alteration bordering deep EDM veins constitutes a singular envelope on veins of quartz, chalcopyrite, and pyrite. At somewhat shallower depth, the EDM alteration per se becomes an outer envelope zone bordering an inner zone of pale green sericite–K-feldspar–chlorite alteration (PGS), and in most cases, magnetite joins quartz, pyrite, and chalcopyrite in the vein assemblage. Such veins are here designated quartz–chalcopyrite–pyrite–magnetite//PGS/EDM (fig. 8C), wherein vein minerals are separated with a double slash from alteration minerals, and a single slash separates alteration zones within the vein envelope (Seedorff and Einaudi, 2004). PGS alteration lacks shreddy biotite and andalusite, but otherwise resembles EDM in containing K-feldspar and sericite replacing granite feldspars, and in displaying sericite island texture (Brimhall, 1977; Roberts, 1975), wherein alteration quartz is separated by K-feldspar from contact with muscovite.

Vein magnetite is conspicuous (fig. 8C), enabling straightforward mapping (Reed, 1979) of the magnetite vein zones (figs. 5, 6, and 9), including in historical samples from the easternmost Leonard mine and in drillholes east of the Continental fault, where the zone outline matches a distinctive aeromagnetic anomaly. Deep drilling in the Pittsmont area and concurrent underground drilling in the eastern Kelley Mine showed that there were two separate domical magnetite vein zones (figs. 5, 6, and 9) that defined the separate Anaconda and Pittsmont domes of the Butte porphyry copper deposit (Reed, 1979). Contemporaneous plotting of molybdenite-bearing veins and Mo assay data outlined the matching moly domes, as depicted in figure 5.

Dark Green Sericitic Alteration (DGS)

Partway outward within the magnetite vein zone, the outer EDM halo of the distinctive PGS/EDM alteration envelopes of magnetite veins is displaced by an outer halo of dark green chlorite with sericite–K-feldspar, DGS, i.e., the PGS/EDM zoned envelope becomes PGS/DGS. DGS is distinguished by the replacement of primary rock biotite by unit pseudomorphs of chlorite, and the absence of shreddy bio-

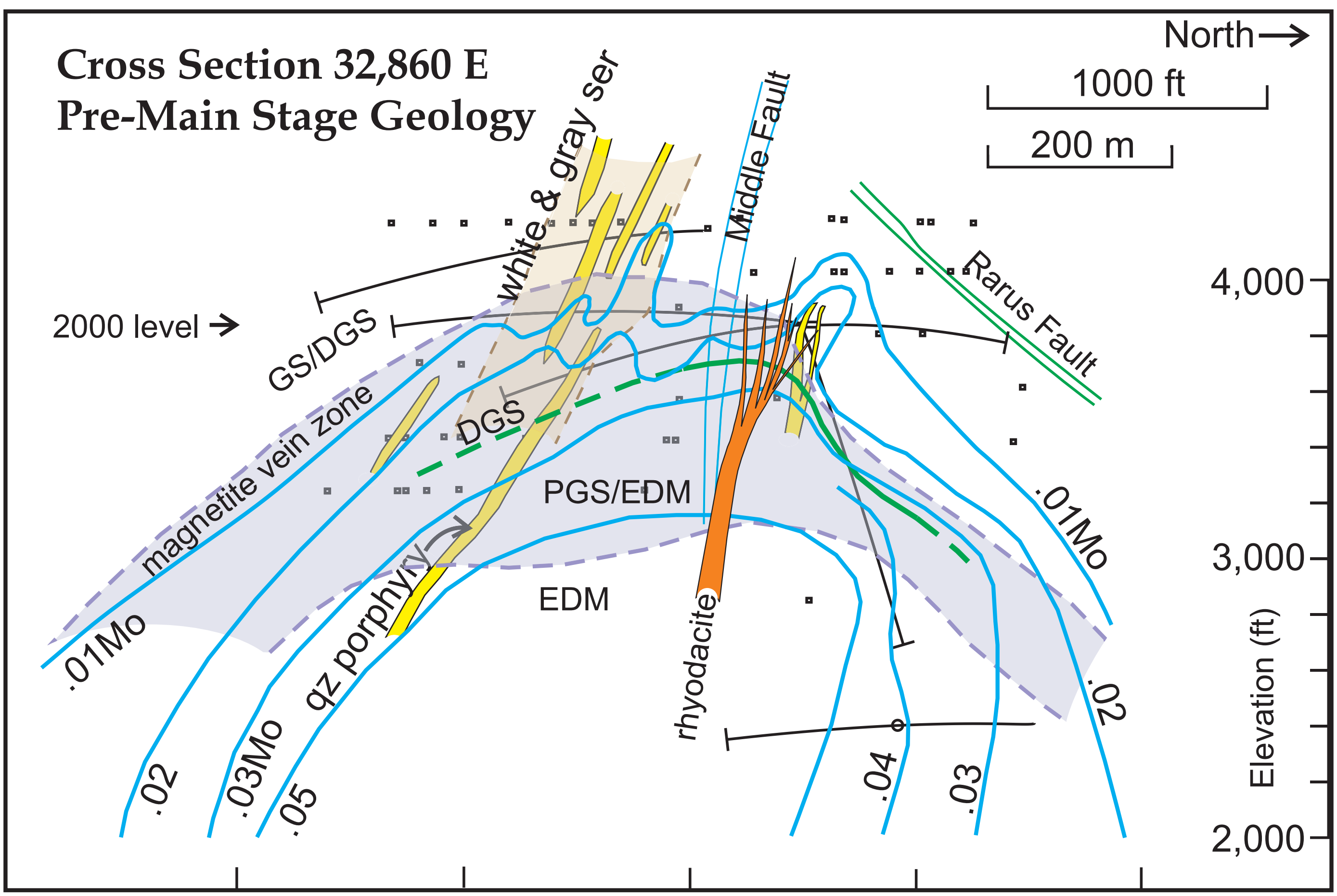

Figure 9. North–south cross section in the eastern part of the Anaconda dome (fig. 5) based on mapping of tunnels (small squares), underground diamond drillholes, and data projected from off-section. The magnetite vein zone is shown in relation to major alteration types: EDM dominantly beneath magnetite veins, PGS/EDM veins in the lower half of the magnetite zone, then an upward transition to PGS/DGS veins above the green contour labeled DGS, and GS/DGS veins above the magnetite zone. Quartz–porphyry dikes are shown in yellow, surrounded by intense white and gray sericitic alteration. Mo concentration is shown in wt%. The east–west rhyolite dike (orange) splays upward into numerous breccia dikes known as the Modoc breccia.

tite. DGS contains fine-grained chlorite, sericite, and K-feldspar replacing feldspars and is distinctive for its dark green color, making it easy to map in drillcore, as shown by the DGS contour in figure 9. The displacement of EDM by DGS constitutes a deposit-scale alteration transition in mafic silicate alteration from biotite-dominant to chlorite-dominant.

In a style analogous to the EDM-only envelopes at depth, DGS-only envelopes occur commonly in the peripheral DGS zone (fig. 9), yielding quartz–pyrite–chalcopyrite//DGS veins (fig. 8E), wherein the DGS is intense, including prominent secondary K-feldspar with sericite and chlorite replacing plagioclase. An outer envelope on many such veins is the same DGS, except that primary granite K-feldspar remains, yielding a distinctive halo of large pink feldspar grains surrounded by chloritized biotite and plagioclase replaced by fine-grained chlorite and sericite (fig. 8E).

Gray Sericitic (GS) Alteration, GS with Remnant Biotite (SBr), and Peripheral Pyritic Veins

Toward the periphery of the magnetite zone, where the amount and grain size of magnetite diminishes, the PGS alteration becomes distinctly pyritic and grayer, and thereby grades into “gray sericitic” alteration (GS), which occurs in GS/DGS envelopes (fig. 8D). In GS-altered granite, feldspars are replaced by sericite, quartz, and pyrite, biotite is pseudomorphed by platy muscovite and large pyrite grains, and K-feldspar is absent. Some biotite is replaced by colorless chlorite (Mg-rich), which is distinguished by its low birefringence and leafy habit and has been verified by XRD (L. Ziehen, oral commun., 1978). In inner GS envelopes, rutile occurs in blocky millimeter-scale grains, but in the outer part of GS envelopes, rutile forms a grid of needles in muscovite pseudomorphs of biotite. The DGS in some distal GS/DGS envelopes lacks K-feldspar but retains sericite and green Fe–chlorite.

In the peripheral zone of pyritic veins (fig. 6) surrounding the Anaconda and Pittsmont domes, the pyrite–quartz//GS/DGS veins are intermingled with similar pyritic veins with GS/SBr envelopes. SBr alteration is the same as GS, except that large biotite grains remain from the original granite with partial fringing replacement by muscovite and pyrite; i.e., feldspars are entirely replaced by sericite, quartz, and pyrite, but primary biotite remains (fig. 8F), creating a distinctive dominantly sericitic alteration speckled with remnant biotite books. The GS/SBr veins are apparently not gradational variants of the potassic series described above, and most resemble the GS/SBr veins of the central gray sericitic zone (fig. 6).

The pyrite//GS veining that is peripheral to the Anaconda and Pittsmont domes is more concentrated along the trace of the quartz porphyry dike swarm, as shown by the distinctly larger volume of GS alteration mapped in the dike corridor revealed in low-angle underground drillholes in the Anaconda dome (fig. 9). The vertically drilled deep holes in the Pittsmont dome do not provide the exposure to document a pyrite//GS overlay on the quartz porphyry dikes in that region; however, a large I-15 roadcut east of the Pittsmont dome contains substantial py-qz//GS veins and a small number of biotite crackles in granite beyond the limit of biotite replacement of hornblende.

Propylitic Alteration

A peripheral zone of propylitic alteration envelopes overlaps and extends beyond the DGS vein zone and is characterized by millimeter-scale quartz–chalcopyrite–sphalerite–galena ± rhodochrosite ± chlorite ± epidote veinlets and crackles each with a propylitic alteration envelope. The alteration consists of epidote, sericite, K-feldspar, chlorite, and carbonate. Propylitic alteration also occurs where epidote augments the outer edges of some distal DGS vein envelopes and occurs outboard from the epidote contour shown in figure 5, which was mapped in Berkeley Pit drillholes by Page (1979), and subsequently extended eastward from deep drilling (Reed, 1979). Propylitic alteration is notably absent from most exposures of Butte Granite cut by EDM and GS alteration zones along I-15 roadcuts east of the Continental Pit (at relatively great paleodepths).

Quartz–Molybdenite Veins

Veins of the potassic series are cut by quartz–molybdenite veins, which are centimeter-scale quartz-dominated veins with small amounts of molybdenite in streaks parallel to the vein walls (figs. 10A, 10F). Quartz–molybdenite veins extend from great depth (sea level) to high in the Pittsmont and Anaconda domes and are conspicuous out to the 0.01 wt% Mo grade contour (figs. 5, 6, 9, 11). Some of the deepest quartz–molybdenite veins in the far eastern area have narrow biotitic or K-feldspar alteration envelopes, but most lack alteration selvages.

In addition to centimeter-scale veins, Proffett (1973) described “banded quartz–molybdenite veins” that are 10–30 cm thick with alternating quartz and

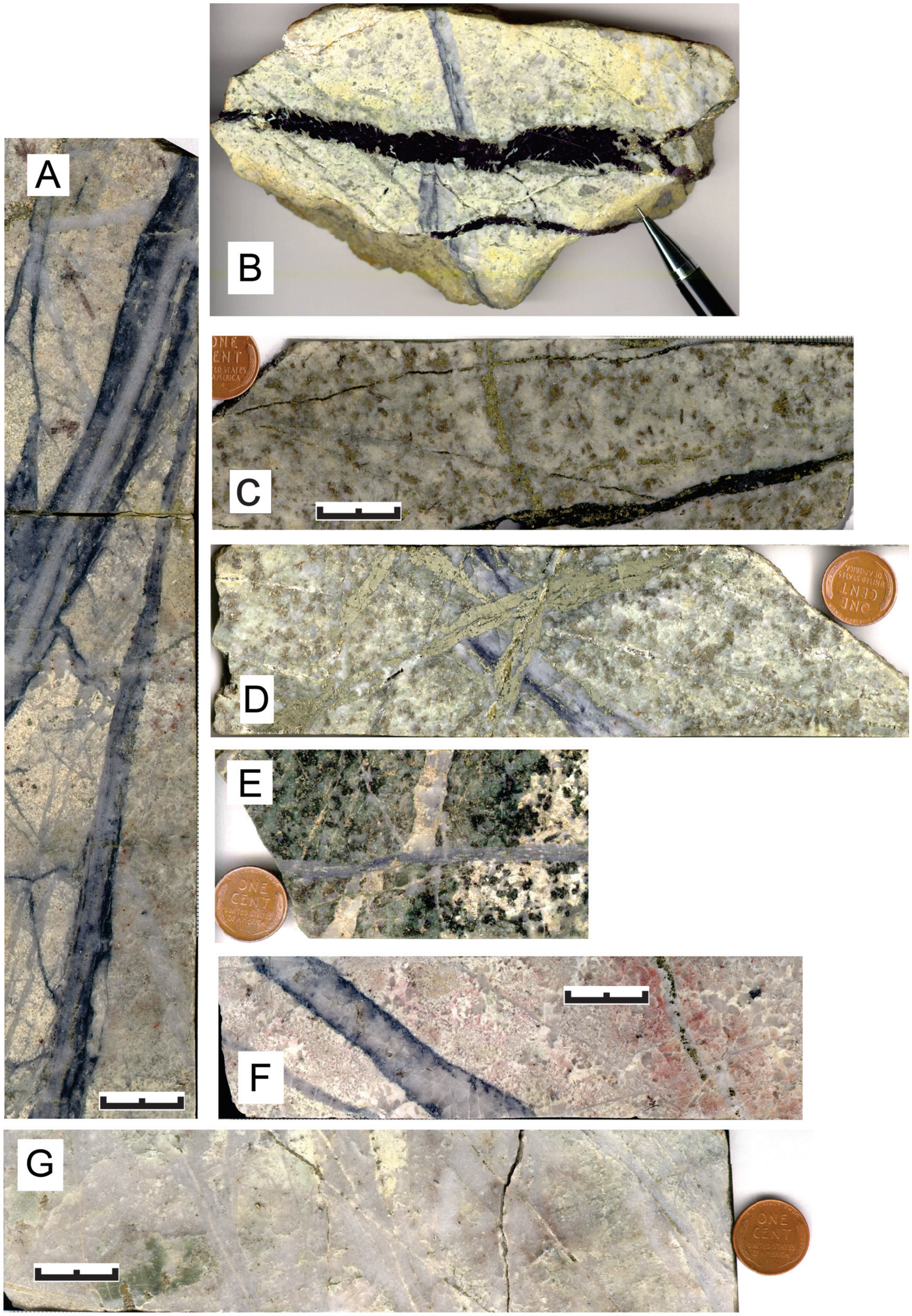

Figure 10. Polished slabs of Butte veins illustrating vein character and cutting relations. Scale bar is 20 mm; coin is 19 mm diameter; all images are at the same scale except B. (A) Banded qz-mb veins cutting small barren quartz vein stockwork, all in aplite dike within the Butte Granite (10969-5699, deep in SW flank of Pittsmont dome). This sample illustrates abundant molybdenite of high-grade Mo zones and the common occurrence of more intense quartz veining in aplite than in adjacent granite. (B) Sericitically altered quartz porphyry cut by an 8-mm quartz–molybdenite vein, which is cut by two covellite–pyrite Main Stage veins (Leonard mine). (C) Intensely GS-altered granite with prominent pyrite replacement of biotite; Main Stage 3- to 8-mm enargite–pyrite vein cuts pyrite–quartz vein (11170-895, center of central GS zone. (D) Intensely GS-altered granite with 4- to 10-mm pyrite vein stockwork cutting a quartz–molybdenite vein (central GS zone, 11052-2719). (E) 7-mm quartz–K-feldspar–molybdenite vein with EDM envelope cut by quartz–molybdenite vein (deep center of Pittsmont dome, 11135-4959). (F) Graphic medium to coarse-grained aplite cut by 12-mm quartz–molybdenite vein. (G) Quartz vein stockwork in intensely sericitized aplite, dusted with fine-grained pyrite and cut by millimeter-scale veinlets of quartz and pyrite with minor sericite (11052-7323, near the end of drill hole 1A, fig. 11).

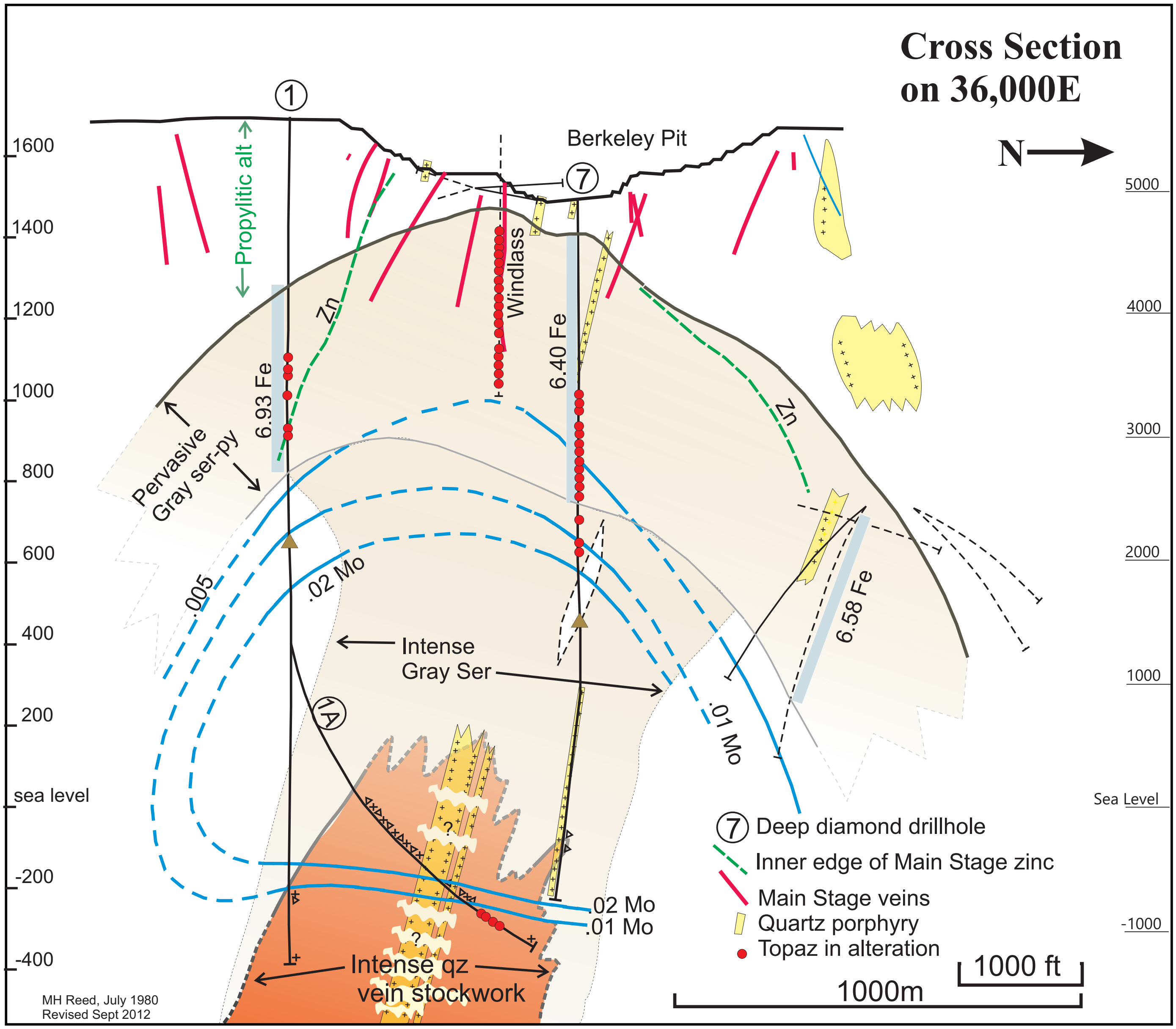

Figure 11. North–south cross section through Deep Holes 1, 1A, and 7 (fig. 5) intersecting the Central GS Zone and the deep quartz vein breccia (Reed, 1979–1981). Diamond drillholes are indicated with curves—solid where they are in the section plane and dashed where near the plane. Vein magnetite (brown triangles) occurs in intervals lacking intense GS alteration. Alteration topaz (red dots) was mapped in the envelope of the Windlass Vein and elsewhere in the pervasively sericitized GS zone and the bottom of DH 1A.

molybdenite layers, and most commonly also laced with banded pyrite of probable late pre-Main Stage origin (see GS below). Proffett (1973) showed in underground mapping from the Anaconda dome that Main Stage fracturing and veins followed many such banded quartz–molybdenite veins, thereby apparently guiding the location and orientation of major Main Stage veins.

Central Gray Sericitic Alteration Zone

Recognition of the central GS alteration zone lying between the Anaconda and Pittsmont domes proved to be one of the most significant findings of the deep drilling project for two reasons: (a) the pyrite–quartz// GS veins of the zone complete the pre-Main Stage vein series, matching the series recognized in other porphyry copper deposits, and (b) its position and rock mechanical properties shaped key structural features of Butte's Main Stage vein system. The geometric center of the Butte District was little known before the deep drilling of the late 1970s. This region—east of the high-grade Main Stage veins of the Belmont, Steward, and Anselmo mines of the old central district, and west of the outlying Pittsmont Mine near the Continental fault—was sparsely traversed by large Main Stage veins only at shallow depths: veins such as the Windlass (fig. 4), characterized by enargite–pyrite bordered by topaz-bearing advanced argillic alteration.

In the first of the deep drillholes, drilled at the southern edge of the Berkeley Pit (DH-1, fig. 11), the upper ~350 m traversed mostly propylitically altered granite, then encountered 450 m of pervasive gray sericitic alteration (GS) in a stockwork of 5- to 15-mm-thick pyrite-dominated veins with minor quartz and chalcopyrite. Bulk rock iron assays in this interval average 6.9 wt% Fe (fig. 11), reflecting the abundance of pyrite in veins and disseminations, compared to less than 4.5 wt% in the non-GS-altered rock above and below the interval. This intense sericite–pyrite alteration intercept was the first of what became recognized as the central gray sericitic zone, an 1,800 m x 1,200 m (at 3,000 ft elevation) domical body with a columnar extension to great depth (Reed, 1979).

The domical top of the central GS zone was defined using direct observations of core and historical samples from crosscuts in the Leonard 3300 and 3800 levels, Kelley 3400, Belmont 3000, Berkeley Pit tunnel (5000 ft elevation), and cuttings from churn drill and rotary drillholes in the Berkeley Pit (Reed, 1979, 1981). Where the boundary of the GS zone was well defined, it followed a distinct positive gravity anomaly, which guided further definition of the GS zone where drilling and mine openings are absent. The gravity high (Wightman, 1979) arises from high density (~2.93 g/cm^3) of the pyrite-rich pervasively GS-altered granite surrounded by low-density (2.72), less-pyritic rock (Reed, 1979).

In much of the central GS zone, the GS vein envelopes on pyrite–quartz veinlets overlap each other, creating pervasive GS alteration (figs. 10C, 10D, 11), but where the pyrite veins are widely enough spaced, an outer envelope of SBr is preserved, wherein primary rock biotite remains (fig. 8F). The central zone pyrite–quartz//GS/SBr veins cut all other vein types except Main Stage (e.g., figs. 10C, 10D).

Gray sericitic alteration of the central GS zone contains the same minerals and destroyed texture as the gray sericitic alteration of GS/DGS veins above the Anaconda and Pittsmont domes (fig. 6), but the central zone GS veins cut quartz–molybdenite veins (fig. 10D), whereas the GS/DGS veins are part of the older EDM-PGS-DGS (potassic) series that is cut by quartz–molybdenite veins.

Deep Quartz Vein Stockwork and Breccia

At depths beneath the central GS zone and beneath the copper and molybdenum mineralization in the Pittsmont dome, deep drilling revealed a massive zone of breccia and stockwork of barren quartz veins (figs. 6, 11). Added quartz veins constitute 15 to 30% of rock volume, as determined by SiO_2 dilution of Ti and Zr in bulk rock analyses. Many of the quartz veins are broken and rotated into breccia fragments, accompanied by quartz porphyry and granite fragments, all of which are suffused with quartz and altered to GS with scattered SBr. The deep quartz zone intercept in DH 1A (fig. 11) also includes a long intersection with quartz porphyry, which is about 100 m thick if it is a steeply dipping dike.

The possible extension of the deep quartz stockwork–breccia beneath the Anaconda dome has not been demonstrated but is suggested by one drillhole beneath the Steward 4200 level where Mo grades decline. The three deep drillhole intersections (DH 1, 1A, 2) suggest that the shape of the top of quartz vein stockwork–breccia could be a choppy east–west surface. This chaotic quartz vein stockwork and breccia zone as a whole consists of about 24 vol% quartz porphyry, 45% granite (and aplite), and 31% nebulous breccia (Reed, 1979). It is unclear how much of the granite and quartz porphyry intersected in drilling consists of large blocks. The brecciation and abundance of quartz porphyry suggests that the zone is part of a cupola at the apex of the magma body that yielded the quartz porphyry dikes of the Butte deposit (Dilles and others, 1999; Reed and others, 2013).

Stable Isotopes of Pre-Main Stage

Studies of stable isotopes of sulfur, oxygen, and hydrogen have been applied by Sheppard and Taylor (1974), Lange and Cheney (1971), Zhang and others (1999), Zhang (2000), and Field and others (2005) to characterize the composition of pre-Main Stage ore fluids. Sulfur isotopic compositions ($\delta^{34}S$) of molybdenite, pyrite, and chalcopyrite range from 3.0 to 4.7‰, 0.4 to 3.4‰, and -0.1 to 3.0‰, respectively, and those of coexisting anhydrite range from 9.8 to 18.2‰. As argued by Field and others (2005), these data suggest that parental porphyry Cu-Mo ores contained more sulfur as sulfate than as sulfide and a bulk $\delta^{34}S$ isotopic composition of about 10‰. The isotopic compositional differences between anhydrite and molybdenite provide estimated equilibrium temperatures of formation of 545–630°C for early porphyry Cu-Mo ores. Oxygen isotope compositions of anhydrite and quartz range from 7.0 to 19.5‰ and 8.9 to 10.0‰, respectively, and are consistent with a magmatic source of fluids. For example, using temperatures of 550–640°C, the calculated $\delta^{18}O$ of the ore fluids is 7.0–8.3‰, which is within the magmatic range of Taylor (1979, 1997).

Weakly altered Butte Granite mafic minerals and pre-Main Stage biotite from potassic alteration and EDM veins, micas, and chlorite from PGS and DGS veins, and muscovite from the gray sericitic alteration (GS), yield oxygen and hydrogen isotopic compositions that are complex and difficult to interpret. Igneous hornblende and biotite in Butte Granite and hydrothermal biotite yield rather typical igneous to high-temperature hydrothermal $\delta^{18}O$ compositions of 4 to 6‰, but yield low δD compositions of -70 to -165‰ (fig. 12). The mineral compositions of hydrothermal biotite (Roberts, 1975; Zhang, 2000) are typical of porphyry copper deposits and formed at 600–700°C (Mercer and Reed, 2013), but these biotite minerals mostly have $\delta^{18}O$ of 5 to 7‰ and δD of -70 to -160‰ that indicate partial oxygen and complete hydrogen exchange with low-temperature meteoric water at about 150–200°C (Zhang, 2000). The isotopic exchange in biotite-rich, PGS, and DGS samples is most pronounced ($\delta^{18}O$ of -2 to 7‰ and δD of -115 to -165‰) in settings where adjacent plagioclase is altered to smectite or kaolinite, the characteristic clays in Main Stage or later green and white argillic alteration, respectively, of intermediate argillic alteration zones (Sales and Meyer, 1948, 1949; Meyer and others, 1968).

Gray sericitic alteration formed at about 400–525°C (Rusk and others, 2008a) and is characterized by muscovite with isotopic compositions of $\delta^{18}O$ of 5.5 to 9.5‰ (one 2.5‰) and δD of -53 to -140‰ (Zhang, 2000). Using a temperature of 400°C for mica–water fractionation equilibration, these muscovite isotopic compositions yield calculated ore fluids with $\delta^{18}O$ of 4 to 8‰ and δD of -24 to -88‰ (Zhang, 2000) that are similar to the range of magmatic fluid compositions and arc magmatic waters, but also extend to lower δD compositions (fig. 12; Taylor, 1979; Giggenbach, 1997). Magmatic isotopic compositions of water have been reported for sericitic alteration elsewhere (Harris and Golding, 2002). The Butte δD compositions of pervasive gray sericite alteration zones are from rather impermeable rocks and therefore were not greatly reset by the low-temperature meteoric waters of the Main Stage or post-Main Stage in comparison to the widely reset pre-Main Stage hydrothermal biotite.

Radiometric Dating of the pre-Main Stage

Isotopic ages for Butte pre-Main Stage hydrothermal minerals suggest the possibility that the Pittsmont porphyry Cu-Mo center formed earlier than the Anaconda porphyry center, which was shortly followed by formation of the central GS alteration zone. Re-Os ages of molybdenite were obtained by Holly Stein at Colorado State University (written commun., 2003; Dilles and others, 2004), and provide several samples with ages of 65.5–66 Ma for the eastern Pittsmont porphyry Cu-Mo center and three samples with ages of 63.4–64.5 Ma for the western Anaconda porphyry Cu-Mo center (fig. 2).

Lund and others (2002, 2018) reported $^{40}Ar/^{39}Ar$ ages of 64–64.5 Ma for several samples of biotite and muscovite from EDM and GS alteration zones in the Pittsmont porphyry Cu-Mo center. A more extensive study by L. Snee (written commun., see also Snee and others, 1999; Dilles and others, 2006) provide several $^{40}Ar/^{39}Ar$ ages for EDM and gray sericite mica samples that are 64 Ma from both the Pittsmont and Anaconda porphyry Cu-Mo centers as well as the large central volume of grey sericite alteration, whereas a few mica samples from the deepest drillholes (1.5 to 2.2 km depth) have younger ages of 61.8 to 62.5 Ma. The latter authors interpret 64 Ma as the age of cooling, following the Butte GS hydrothermal event, below about 300–350°C, the closure temperature for Ar gas diffusion in muscovite and biotite. Ages younger than 64 Ma likely were produced by Main Stage heating (220–330°C; Rusk and others, 2008b; Miller, 2004; Ortelli, 2015), or by the 60–61 Ma rhyodacite dike.

MAIN STAGE VEIN SYSTEM

Metal Zonation and Sulfides

Geologic studies of the Butte Main Stage vein system provided one of the world's first portrayals of metal zoning and vein paragenesis in lodes (veins >1 m wide) with >2 km strike length. The giant Butte Main Stage vein system (figs. 3, 4) was recognized early (Weed, 1897) for its size and well-defined zoning of metals. Three crudely concentric ore zones were defined by Reno Sales (1914, p. 58): (1) the Central Zone (copper), "in which the ores are characteristically free from sphalerite and manganese minerals"; (2) the Intermediate Zone (copper–silver–zinc–manganese), "in which ores are predominantly copper, but are seldom free of zinc;" and (3) the Peripheral Zone "in which copper has not been found in commercial

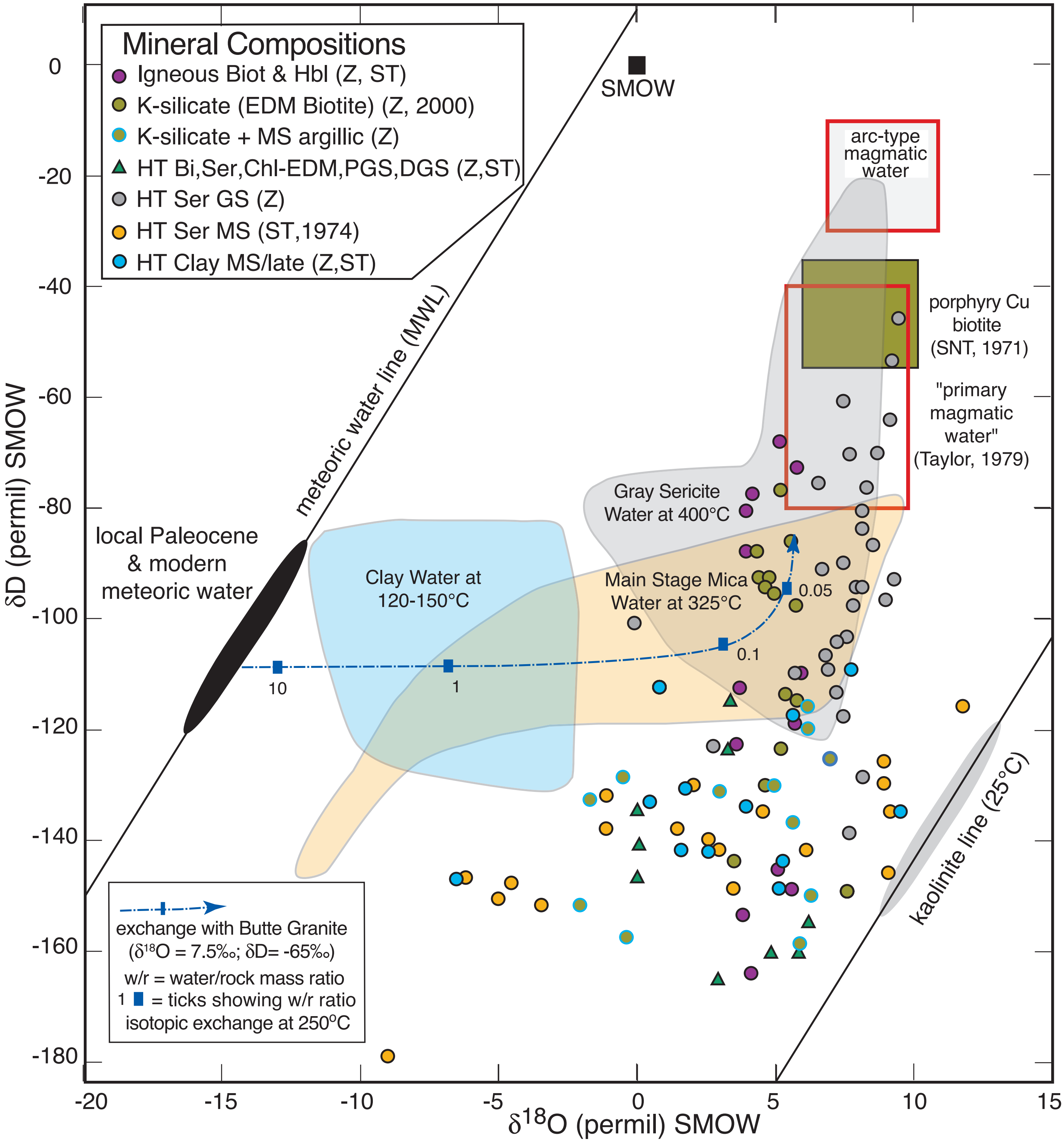

Figure 12. Oxygen and hydrogen isotopic compositions of Butte Granite, pre-Main Stage minerals, and Main Stage minerals, together with calculated isotopic compositions of fluids responsible for pre-Main Stage gray sericite, Main Stage micas, and Main Stage to late clays (smectite, kaolinite). Meteoric and magmatic waters together with 25°C kaolinites produced by weathering are from Taylor (1979) and references therein. The porphyry–copper biotite field of Sheppard and others (1971) and arc magmatic water fields are shown for comparison. Water-rock reaction paths of Paleocene waters with Butte Granite are calculated using the methods outlined in Taylor (1979). Water compositions were calculated from mica and clay-water fractionation factors for oxygen and hydrogen (Zheng, 1993; Vennemann and O'Neil, 1996; Gilg and Sheppard, 1996). Isotopic data are compiled from Sheppard and others (1969), Sheppard and Taylor (1974), and Zhang (2000).

quantities." The Peripheral Zone was principally mined for silver, zinc, and lead, but also for manganese in rhodochrosite–rich veins such as the Emma–Travona (Meyer and others, 1968). Individual veins or vein systems in many cases display this full metal zonation on the scale of more than 100 m, such as the Anaconda–Steward–Original–Gambrinus (fig. 4). Details of vein mineral zoning, including maps, and the transitions from copper- to zinc-rich ores by outward and upward zonal advance of copper into zinc, were described by Meyer (Sales and Meyer, 1949; Meyer and others, 1968).

The principal zonation of vein minerals is from pyrite–enargite–chalcocite–covellite in the Central Zone outward to pyrite–bornite–chalcopyrite–chalcocite with minor sphalerite and tennantite in the Intermediate Zone to rhodochrosite (or rhodonite)–sphalerite–galena–pyrite in the Peripheral Zone (fig. 13). Meyer and others (1968) also document the "deep chalcopyrite-rich zone," which lies below the Intermediate Zone, and is characterized by pyrite–chalcopyrite–bornite–tennantite. The sulfidation state or sulfur/metal ratio increases upward from the deep chalcopyrite zone to the Intermediate Zone and decreases outward from the Central Zone towards fresh rock in all directions. Meyer and others (1968) ascribed the outward decrease of sulfur/metal ratio to wall-rock buffering. Deep drilling and mining since 1968 have enabled small additions to the metal zoning maps (fig. 4), particularly an interior boundary of zinc-rich veins in the south-central and Pittsmont regions.

Main Stage vein mineral paragenesis is complex and incompletely known, and early studies summarized by Meyer and others (1968) describe an early sphalerite–quartz–pyrite stage that is replaced and cut, except for a few local reversals, by copper-rich minerals, and that sphalerite and enargite are generally replaced by digenite–bornite–chalcopyrite–tennantite (fig. 13, table 4). There is an antithetic relationship of chalcopyrite to chalcocite–digenite, where the former dominates the deep-chalcopyrite zone, and chalcocite–digenite mixtures dominate shallow zones. Rhodochrosite occurs with sphalerite but also overgrows sphalerite in vein breccias of the Peripheral Zone.

Detailed paragenetic studies by M. Ortelli (Ortelli and others, 2013, 2015; Ortelli, 2015) on a more limited sample set provide many observations of vein mineralogy and associated fluid inclusion pressure, temperature, and composition. Also, Gammons and others (2016) provide mineralogical details of silver in the Main Stage. Ortelli's studies describe a four-stage age progression for veins in the Central, Intermediate,

Table 4. Main Stage vein mineralogy and wall-rock alteration zones.

	Central Zone (Advanced Argillic)	Central Zone (sericitic)	Intermediate Zone	Deep Level Chalcopyrite Zone	Peripheral Zone	Post-MS Argillic
Metals	Cu(Ag)	Cu(Ag)	Cu(Ag,Zn)	Cu(Ag)	Zn-Mn-Ag (Pb,Cu)	—
Sulfide & ore minerals	py-cc-cv-dg-dj-en-(bn)	py-cc-bn-en (cls,dg,cv)	py-bn-cp-cc-(tn,sl)	py-cp-bn-tn(cc,en)	rc-rn-sl-gn-py (cp,tn,ac)	py
Gangue in vein	qz (alunite)	qz	qz(cal,dol,fl)	qz(cal,dol)	qz,cal,dol (chalced,ank,ap,fl)	cal
alteration:						
Innermost vein margin	kln,dck, prl, tz (zunyite)					
Main sericite zone	ser (2M ms)	ser (2M ms)	ser (2M ms)	ser (2M ms) ser-K-feld (edge of cp Zone)	ser (2M ms) narrow	mnt/ kln
Outer	—	—	mnt/kln	mnt/kln	mnt/kln	
Outermost	—	—	Propylitic	Propylitic	Propylitic	

Note. Minerals listed are very abundant, abundant, or common, and those (in parentheses) are minor. Trace and rare phases are not listed (simplified from table 1 of Meyer and others, 1968).
ac, acanthite; ank, ankerite; ap, apatite; bn, bornite; cal, calcite; cc, chalcocite; cal, calcite; chalced, chalcedony; cls, colusite; cp, chalcopyrite; cv, covellite; dg, digenite; dck, dickite; dj, djurleite; dol, dolomite; en, enargite; fl, fluorite; gn, galena; kln, kaolinite; mnt, montmorillonite; ms, muscovite; py, pyrite; prl, pyrophyllite; qz, quartz; rc, rhodochrosite; rn, rhodonite; sl, sphalerite; ser, sericite; tn, tennantite; tz, topaz.

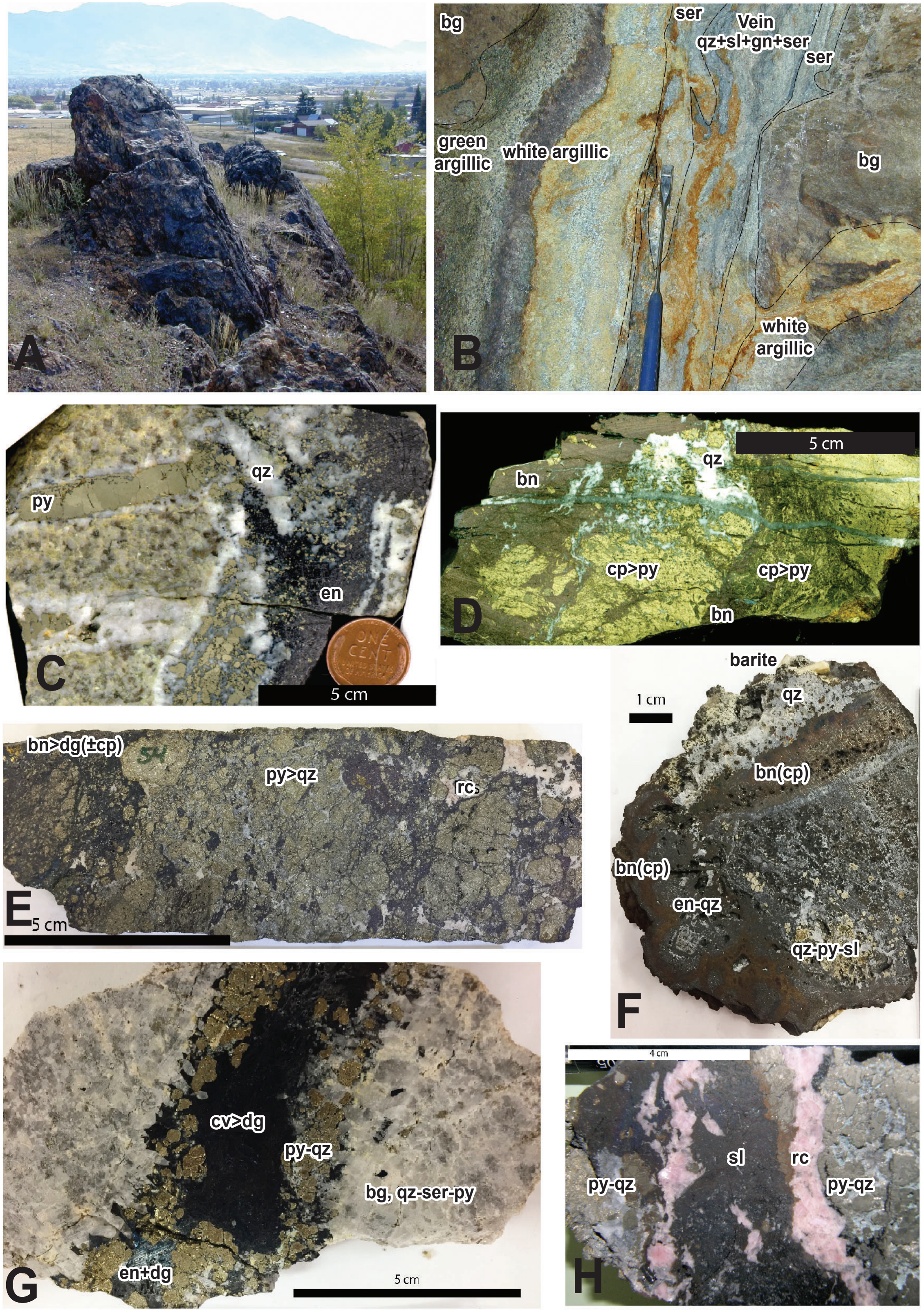

Figure 13. Photographs of Main Stage veins, illustrating vein mineral assemblages. (A) Prominent Mn-oxides (black) and quartz of Emma Vein, 2–3 m wide, looking southwest (Peripheral Zone). (B) Quartz–sphalerite–galena fault vein (Lexington tunnel, Peripheral Zone) containing sheared wall rock and having a narrow sericitic alteration selvage. Note that the white and green argillic selvages are asymmetric and not present on the upper right part of vein, suggesting they postdate vein and sericite formation. (C) Enargite–pyrite–quartz vein cutting pyrite–quartz//GS vein (GRL 10883-7, Berkeley Pit). (D) Massive chalcopyrite–pyrite partially replaced by bornite (X3677, Mt. Con 4000 level, Syndicate Vein). (E) Brecciated pyrite and quartz infilled with bornite–digenite (chalcopyrite) and late rhodochrosite. (F) Early quartz–pyrite–sphalerite overgrown by enargite–quartz, enclosed in bornite (chalcopyrite) and late quartz-rich vein with barite (GRL-3016). (G) Vein cutting sericite–pyrite altered Butte Granite (Central Zone). Note outer vuggy quartz–pyrite zone and overgrowth of enargite–digenite, with late infill of covellite–digenite. (H) Early pyrite vein infilled with sphalerite and coarse rhodochrosite (Peripheral Zone).

and Peripheral Zones (Ortelli, 2015): (a) early quartz–sphalerite(I)–(pyrite–galena) with sericite, is cut by (b) quartz–pyrite–enargite with sericite ± dickite, in turn cut by (c) sphalerite(II)–pyrite–chalcopyrite–tennantite–rhodochrosite (minor sericite), and in the Central Zone cut by (d) pyrite–covellite–digenite–bornite (pyrophyllite). Fluid inclusion measurements indicate 1–6 wt% salinities and low pressures (60–220 bars), and temperatures that decline from highs of 280°C to 320°C in stages (a) and (b) in the Central and Intermediate Zones to as low as 190–210°C in stage (c) sphalerite–rhodochrosite from the Emma Mine in the Peripheral Zone. These data generally support the early interpretation that the Main Stage veins formed from a succession of ore fluids containing silica, Fe, Cu, Zn, Pb, Ag, Mn, and As that produced metal zoning upward and outward in an evolving temporal progression (Sales and Meyer, 1949).

Wall-Rock Alteration

In a classic study (Sales and Meyer, 1948), Meyer described Main Stage veins with zoned alteration envelopes (fig. 13) bordered by an inner zone of sericitic alteration, followed outward by intermediate argillic alteration, and an outer zone of propylitic alteration developed against fresh rock. The sericitic alteration is characterized by centimeter- to 10-m-wide envelopes in which K-feldspar and plagioclase have been converted to fine-grained (10–100 mm) white mica and lesser quartz, and biotite and hornblende are replaced by white mica, quartz, pyrite, and rutile with local pale chlorite. Mica compositions span the range from muscovite to illite, consistent with formation at 250–350°C. Pervasive alteration forms by overlapping of narrow selvages on closely spaced veins, particularly in the Central Zone near major vein intersections and along horsetail veins of the Leonard—Belmont axis (Meyer and others, 1968; Gustafson, 1973; Thompson, 1973) but some pervasive sericitic alteration in Central Zone originates from the older central GS zone. Many veins that contain covellite–enargite–digenite–pyrite in the Central Zone (Leonard, Tramway, Berkeley mines) also contain alunite and have an innermost zone of advanced argillic alteration consisting of pyrophyllite, dickite or kaolinite, sericite, topaz, and quartz. At depths greater than 1,000 m, advanced argillic alteration contains pyrophyllite, topaz, and local zunyite and dickite. The sericitic envelopes diminish in width westward and are generally narrower along Blue Veins compared to Anaconda Veins. In the Intermediate Zone, envelopes are narrower (<30–60 cm) than the veins they border, and in the Peripheral Zone are still narrower and contain chlorite (<1–10 cm in the Orphan Girl to Blue Bird mines). In the northern part of the Peripheral Zone, these narrow sericitic selvages contain K-feldspar.

Distant from the central GS zone, where Main Stage veins are surrounded by nearby fresh granite, the inner sericitic zone is always surrounded by a narrow zone (~1–30 cm) of intermediate argillic alteration, and an outer propylitic zone containing minor chlorite, smectite, epidote, and sparse carbonate minerals. Sales and Meyer (1948) divided the intermediate argillic zone, where mixed-layered clays preferentially replaced the more calcic plagioclase, into an inner "white argillic" subzone containing kaolinite after plagioclase, altered hornblende sites, and relict igneous K-feldspar and biotite, and outer "green argillic" subzone containing smectite, hornblende, and biotite altered to smectite–chlorite, and relict igneous biotite. Similar smectite–rich and local kaolinite-rich alteration is otherwise widely distributed in the district throughout the pre-Main Stage potassic alteration zones of the Pittsmont and Anaconda domes along post-ore faults, many of which follow Main Stage veins but do not always form symmetric alteration envelopes, and replacing post-ore rhyodacite dikes. Stable isotopic compositions of clays (see below) and the 200°C upper-temperature limits of kaolinite and smectite in geothermal–epithermal systems (Simmons and others, 2005; Reed, 1994) suggest that much of the intermediate argillic alteration formed later and at lower temperature (120–150°C) than Main Stage veins.

Main Stage Structural Pattern

The Main Stage vein system occupies two fault systems termed the Anaconda Veins by Meyer and others (1968) and Proffett (1973; Steward Veins of Lund and others, 2018) and the Blue Veins by Meyer and others (1968). As summarized by Houston and Dilles (2013a), the Anaconda Veins strike N 60–70°E and dip steeply (generally 75–90°S, but becoming steeply north-dipping at depth near sea level), whereas the Blue Veins strike N 50–55°W and also dip steeply south (75–90°). Both vein sets form ores, and hydrothermal vein fillings range from nil to several meters. Each of these fault/vein sets mutually offsets the other one locally, and contains the same vein fill and hydrothermal alteration minerals; therefore, the two vein sets formed synchronously (Meyer and others, 1968; Proffett, 1973). Fault offsets along these veins documented in underground mapping range from ~1 m up to 34 m for the Anaconda Veins (Proffett, 1973) and up to ~100 m on the Blue Veins (Sales, 1914). No faults have large displacements.

Anaconda Veins display a combination of right-slip and normal offset, whereas Blue Veins display a combination of left-slip and normal offset (Proffett, 1973). Most of the veins contain fault breccias with hydrothermal healing, and many veins are faulted, post-ore and these zones commonly display clay alteration in wall rocks as does the 60–61 Ma rhyodacite dike. Both Proffett (1973) and Houston and Dilles (2013a) conclude that the Main Stage veins formed as a result of minor east–west shortening consistent with a maximum principal stress oriented N 80°W–S 80°E and least principal stress oriented N 10°E–S 10°W. The Anaconda Vein, the thickest in the district, averages 6 to 10 m wide and is up to 30 m in places (Meyer and others, 1968). It strikes N 80°W and therefore has an orientation consistent with being a tensional fracture in this stress field. The east–west shortening documented for the Anaconda and Blue Veins is consistent with the Laramide shortening direction in the southwest Montana fold and thrust belt. Houston and Dilles (2013a) proposed that the Main Stage faults resulted in both minor east–west regional shortening and north–south extension, both of which were focused in the brittle crust overlying the deep porphyry magma chamber. The extension was possibly produced by buoyancy and minor ascent of the deep volatile-saturated magma.

Relationship of Main Stage Veins and Advanced Argillic Alteration to the Central GS Zone

Fracturing in response to the regional stress environment examined above was shaped on the district scale by the central GS zone. Main Stage veins such as the Anaconda–Steward, Syndicate, State, and Black Rock and many more are thick and long in the western part of the district, but most veins and workings on them end eastward where they intersect the central GS zone. A few veins cross the zone at shallow depth (e.g., 1500 mine level map in Sales, 1914), and only the Windlass Vein crosses at intermediate depth (e.g., 3,400 ft elevation; figs. 4, 14). The coincidence of the lack of Main Stage veining with the central GS zone became clear when the contours of the GS zone were superimposed on maps of Main Stage veins by Meyer and Reed (Reed, 1979), revealing (figs. 4, 14) that vein ores in the Steward, Kelley, Leonard, and Belmont mines end eastwardly where they reach the GS zone. On the east side of the GS zone, Main Stage veins reappear in the Pittsmont Mine.

Veins within the GS zone such as the Windlass (figs. 11, 14) and horsetails of the deep Leonard are bordered by intense advanced argillic alteration characterized by topaz, zunyite, pyrophyllite, kaolinite, and quartz. In earlier studies, the location of this advanced argillic alteration was credited to pervasive Main Stage sericitic alteration around the horsetail ores, but with the recognition of the central GS zone, it now appears that much of the advanced argillic alteration is a consequence of acidic Main Stage fluids reacting with already-sericitized rock of the GS zone, which failed to neutralize the acidity.

Meyer and others (1968) pointed out that Sales' (1914) "central zone" ore minerals and Meyer's "high-sulfur assemblage" of covellite–digenite–enargite–pyrite overlap with advanced argillic alteration. Both occur where intense Main Stage fluid penetration intersected the already-existing zone of GS alteration, which allowed the acidic fluids to remain acidic, thereby producing the high-sulfur assemblage (e.g., Reed and Palandri, 2006). The occurrences of the high-sulfur assemblage and topaz alteration in and bordering Main Stage veins such as the Windlass (fig. 4) and in Deep Drill Holes 1 and 7, which penetrate the full thickness of pervasive GS alteration (fig. 11), also reflect the chemical association of advanced argillic alteration with high-sulfur minerals long recognized in the Leonard mine, and in high-sulfidation epithermal deposits worldwide.

Horsetail Fracturing Bordering the Central GS Zone

The central GS zone formed in the late pre-Main Stage, as demonstrated by several 64 Ma $^{40}Ar/^{39}Ar$ ages on sericite (muscovite) of the GS, and by vein cutting relations—pyrite//GS veins cut quartz–molybdenite veins and are cut by Main Stage veins (fig. 10). At the time of Main Stage fracturing, the relatively ductile rock of the central GS zone was surrounded by fresh granite and pre-Main Stage-altered granite, both of which were feldspar-rich, making them brittle. Main Stage strain fractured the brittle ground distal to the GS zone, producing throughgoing fissures east and west of the central GS zone, but not in the ductile GS-altered rock (fig. 14).

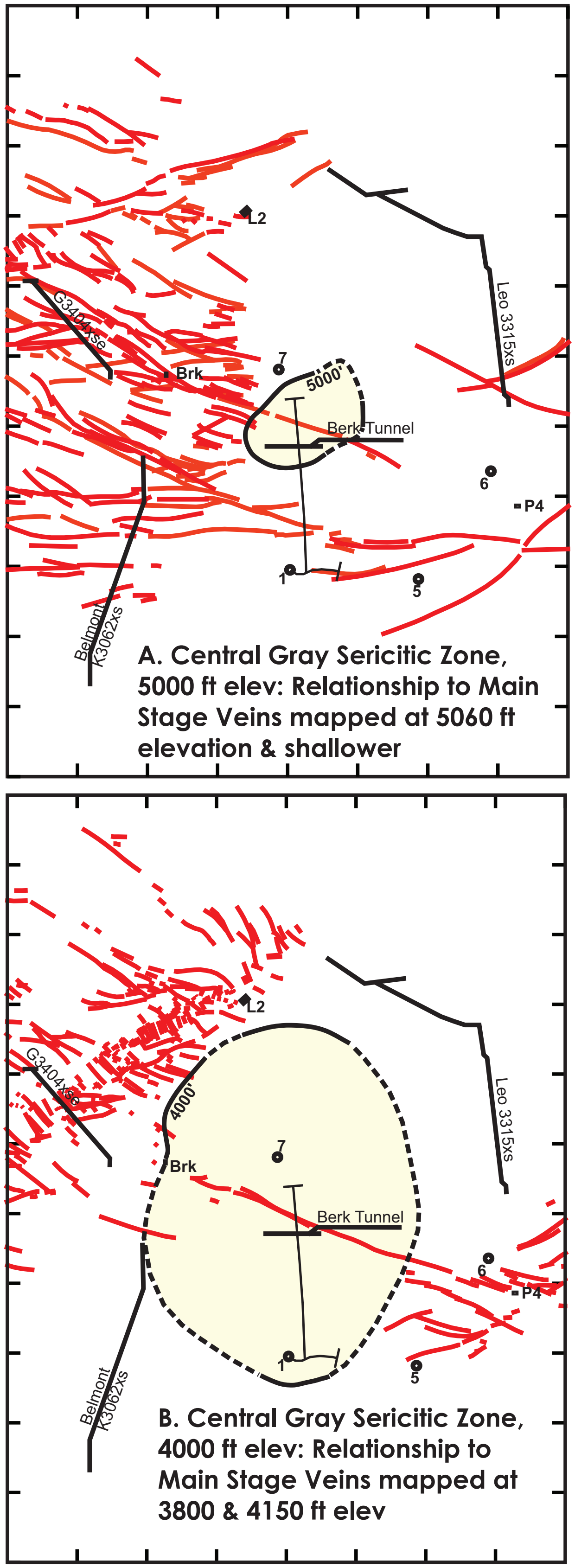

Figure 14. Central Gray Sericitic Zone in relation to Main Stage Veins. (A) Main Stage veins above 5,000 ft elevation shown in relation to the top of the GS Zone. Veins traverse through unsericitized ground above the GS zone, which expands beneath 5,000 ft. (B) Veins near 4,000 ft elevation, which are numerous to the west of the GS Zone and in the Pittsmont mine to the east, but only the Windlass cuts through the zone, where it contains minerals of the high-sulfur assemblage (pyrite, enargite, digenite, covellite) and is bordered by advanced argillic alteration, with characteristic topaz, shown in figure 11. Horsetail vein sets are visible to the northwest and north of the GS zone in map B. Also visible, wrapping around the GS zone from its western margin northward, is a gradational change in the strikes of veins of all kinds from east–west and west–northwest for the more southerly veins in the west to nearly north–south for the veins in the north.

The horsetail veins of the Leonard and Tramway mines are small, closely spaced, southeast-striking fractures that break away from east–northeast-striking large veins, forming an *en echelon* vein set (Meyer and others,1968). The elongate direction of the horsetail veins as a set strikes in about the same direction as the east–northeast large veins. It is likely that the particular location of horsetail veins was fixed by the transition in rock mechanical properties along the northwest flank of the central GS zone (figs. 4, 14) where ductile GS-altered rock transitions to brittle fresh granite (Reed, 1979, 1981). Horsetail fractures formed where throughgoing fissures in brittle rock broke into a series of *en echelon* tears near the GS boundary because the shear strain focused in the large vein fracture was spread over a large volume in the ductile GS zone.

The macroscopically ductile behavior of the GS-altered granite is expressed in the form of strain on closely spaced small fractures that produced millimeter- to centimeter-scale veinlets of chalcocite, bornite, or enargite within the pervasive GS (DH-1, 1A, 7; fig. 11), some of which have adjacent topaz alteration. Except in the Windlass vein, fluids were not channelized in large fractures, which did not exist. Main Stage hydrothermal fluids also permeated the GS alteration at the grain scale, as indicated by bornite and chalcocite disseminations in the pervasive GS zone, much of which replaces disseminated chalcopyrite, revealed by widespread chalcocite and bornite rims on chalcopyrite.

Stable Isotopes of the Main Stage

The oxygen and hydrogen isotopic compositions of the micas and clays in the Main Stage alteration zones span a large range and were used in early studies by Sheppard and others (1969, 1971) and Sheppard and Taylor (1974) to suggest that fluids were mixtures of dominantly meteoric and minor magmatic waters. They reported $\delta^{18}O$ of quartz from -2 to +12.5‰. Using fractionation factors of Sharp and others (2016) and an inferred temperature of formation of 325°C, these values yield estimated water compositions ranging from -8 to +6.5‰ and reflect a range of dominance from meteoric water to magmatic waters, respectively. Ortelli (2015, p. 162) analyzed early-stage and late-stage quartz and calculated $\delta^{18}O$ of water of 12.2‰ for early quartz and -3 to -9‰ for late quartz, which suggests a shift in dominance from early magmatic to late meteoric waters. The Main Stage micas are chiefly muscovite and minor illite and pyrophyllite, and these have δD compositions ranging from -115 to -152‰ (Sheppard and Taylor, 1974) that provide calculated water compositions at 325°C that range from -80 to -120‰ and reflect a mixture of meteoric and magmatic components (fig. 12). The kaolinite from the post-ore 60–61 Ma rhyodacite dike in the Orphan Girl also has a low $\delta^{18}O$ of 3.9‰ and low δD of -134‰ (Sheppard and others, 1969), which supports incursion of post-ore meteoric-dominated fluids at T <200°C (fig. 12, 120–150°C).

Stable isotope measurements on Main Stage vein carbonates (Garlick and Epstein, 1966; Stevenson, 2015) also suggest that oxygen is derived from mixtures of magmatic and meteoric waters, and carbon is likely derived from oxidized (carbonate) magmatic sources that commonly have $\delta^{13}C$ of -10 to 2‰ (Ohmoto and Rye, 1979). The $\delta^{13}C$ and $\delta^{18}O$ of rhodochrosite ranges from -8.3 to -2.9 and -1.8 to 12.8‰, respectively, whereas $\delta^{13}C$ and $\delta^{18}O$ of calcite ranges from -9.0 to -2.6‰ and -4.4 to 12.3‰, respectively (Stevenson, 2015).

Sulfur isotopes of the Main Stage were reported by Lange and Cheney (1971) and Field and others (2005). Main Stage sulfides (n = 28) range from -3.7 to 4.8‰. Calculated $\delta^{34}S_{H_2S}$ of fluid for these two stages ranges from 0 to 2‰ and, when combined with an unknown amount of ^{34}S-enriched sulfate, the bulk fluid $\delta^{34}S_{SS}$ for late moderate to low-temperature fluids was >2‰.

Age of the Main Stage Veins and Alteration

The age of the Main Stage veins and ores remains somewhat uncertain, but on the basis of complex geochronology, it formed between 64 and 62 Ma, and we consider an age of 63.5 to 63 Ma to be most likely, as discussed below. In the central Butte District, the age of Main Stage, as constrained by geologic relationships, is based on veins that cut the Modoc porphyry and are in turn cut by the rhyodacite dike, which have reliable U-Pb zircon ages of 66 ± 1 Ma and 60–61 Ma, respectively (fig. 2).

The interpretation of the $^{40}Ar/^{39}Ar$ isotopic ages for muscovite (sericite) in Main Stage vein selvages remains controversial because few samples yield robust weighted mean plateaus that provide straightforward age interpretation. Moreover, micas (muscovite, biotite) have relatively low closure temperatures of 300–350°C, and K-feldspar lower closure temperatures of ~180°C, depending on cooling rates. Both minerals are susceptible to thermal resetting.

Lund and others (2018) reported many Main Stage muscovite ages of 67–75 Ma from the periphery of the Butte District, and on this basis proposed a ~72–73 Ma age for these Ag-Au veins containing rhodochrosite, sphalerite, and galena. These ages are substantially older than the Butte porphyry Cu-Mo ores in the center of the district but are similar to 74–75 Ma polymetallic veins in the central Boulder Batholith (fig. 2) that have a cumulative production less than 10% of Butte Zn-Pb-Ag-Mn veins. For example, the largest production is 3,478 t Cu, 14,557 t Zn, 26,544 t Pb, 349 t Ag, and 3.7 t Au from the Jefferson City quadrangle from quartz veins with sericitic selvages containing tourmaline, pyrite, sphalerite, galena, arsenopyrite, and minor tetrahedrite (Brecraft and others, 1963). The veins differ from the Butte Main Stage by a lower Ag/Au ratio (94 compared to 230), presence of arsenopyrite and tourmaline, and paucity of rhodochrosite. While the Lund and others (2018) hypothesis of Butte Ag-Pb-Zn-Mn vein formation at ~72–73 Ma remains to be tested thoroughly, we suggest that most of these ores were introduced during a post-64 Ma Main Stage event that was strongly zoned from inner Cu(Ag) to Cu-Zn(Ag) and peripheral Ag-Pb-Zn-Mn (Weed, 1912; Sales, 1914). Below, we summarize supporting evidence.

Ortelli (2015) provided a detailed vein paragenesis from several samples of the Main Stage, and demonstrated that rhodochrosite–sphalerite–galena ores both predate and postdate copper sulfide (enargite–digenite–bornite) in the intermediate zone. Snee and others (1999) reported $^{40}Ar/^{39}Ar$ white mica ages from Main Stage selvages that range from ~64 to ~62 Ma, and include robust plateau ages of 63.8 ± 0.4 Ma and 63.3 ± 0.2 Ma of two samples from the Emma Vein in the peripheral Zn-Pb-Ag zone (fig. 2). These are similar to four ages of ~64 Ma determined by Lund and others (2018) from the Leonard–East Colusa–Steward mines in the Cu-rich Central Zone area. Snee and others (1999) also reported an $^{40}Ar/^{39}Ar$ plateau age of 62.8 ± 0.2 Ma from the Belmont Mine of the Central Copper Zone, and the youngest $^{40}Ar/^{39}Ar$ ages of 61–63 Ma at Butte from muscovite and K-feldspar in Main Stage veins and muscovite–topaz-bearing alteration zones from the deep drillholes at 1.5–2 km below the surface. These data suggest that preservation of 73–74 Ma $^{40}Ar/^{39}Ar$ sericite ages of Lund and others (2018) occurred only in the Peripheral Zone where 64–62 Ma Main Stage rhodochrosite–galena–sphalerite veins formed by near-neutral carbonate-rich fluids that did not make new sericite, and that were sufficiently low in temperature (~220–330°C) that older mica ages were not reset.

The current geochronology suggests that formation of the central gray sericite alteration zone at 64 Ma, and cooling below 350°C, was followed by brittle faulting and fracturing of rock and Main Stage vein formation (Houston and Dilles, 2013a; Tosdal and Dilles, in press). Most central district Main Stage $^{40}Ar/^{39}Ar$ mica ages are 63–64 Ma, but several ages of micas and K-feldspar are 61–63 Ma and indicate a younger thermal event. The younger ages of several deep sericite samples with low closure temperatures (350–300°C) and K-feldspar (~180°C) are consistent with partial thermal resetting by the 60–61 Ma rhyodacite porphyry dike that is widely altered to kaolinite- and smectite-rich clays and minor pyrite (fig. 2).

SUPERGENE COPPER MINERALIZATION

Weathering of primary ores has played an important role in Butte mining and exploration. Marcus Daly and George Hearst recognized the potential of the gossan of Anaconda vein outcrops and paid $30,000 for it in 1881 despite the outcrops being barren of copper at the surface. Daly's shaft encountered leached vein to 150 m depth and rich copper ore at 180 m below surface. Where first encountered, much of the copper occurred as supergene chalcocite deposited atop hypogene mixtures of pyrite, digenite, covellite, and enargite. Supergene processes also produced silver-enriched zones containing argentite (Ag_2S) and stromeyerite (Ag_2S-Cu_2S), which occurred both with supergene chalcocite and primary enargite in the central zone as well as in early silver-rich ores mined in the Peripheral Zone of the Main Stage veins (Gammons and others, 2016). Supergene oxidation also converted rhodochrosite-rich ores, the main source of past manganese production, in the Peripheral Zone to manganese oxides, principally cryptomelane and psilomelane (Meyer and others, 1968).

McClave (1973) reviewed supergene copper ore that constituted a large part of the production from the Berkeley Pit, which principally mined closely spaced but narrow Main Stage veins (including the horsetail zones) from the Cu-rich Central Zone. By 1978, mining in the Berkeley Pit reached the top of the pre-Main Stage pervasive GS alteration below the Butte Hill, where there was less enrichment. The supergene leached zone in Main Stage veins and along additional permeable faults extended from 30 to >160 m depth and was characterized by goethite-rich limonite, jarosite, and other oxide minerals (Guilbert and Zeihen, 1964). The supergene ore beneath consists largely of sooty fine-grained "chalcocite" and traces of covellite coating pyrite and both coating and replacing bornite–chalcopyrite (the former a likely Main Stage mineral), whereas primary Main Stage digenite and enargite were largely preserved (McClave, 1973). Supergene chalcocite was accompanied by minor uraninite, revealed by K-U-Th gamma logging of exploration holes between the Berkeley Pit and the Continental fault. The supergene blanket averaged 0.75 wt% Cu and 53 m thickness in the Berkeley Pit and lesser thicknesses extended east and southeast beneath gravels to the Continental fault on the west margin of the Continental Pit, and constitute a significant current resource.

The blanket was irregular in thickness and extended to more than 350 m depth along the Middle fault, and to >100 m along Main Stage veins and the Rarus fault, apparently because of the enhanced permeability of these zones. The age of supergene enrichment is poorly constrained, but likely dates from uplift of the Butte deposit to the surface concurrent with eruption of the 48–52 Ma Lowland Creek Volcanics (Houston and Dilles, 2013a). The northwest-striking Middle and Rarus normal faults likely formed at this time, and supergene zones along the faults must, therefore, postdate 52 Ma. The supergene blanket between the Berkeley and Continental Pits is buried beneath 100–200 m of water-saturated Quaternary(?) gravels that postdate supergene enrichment. The gravels were deposited on the downthrown or hanging wall of the Continental fault, which has been active from the Miocene (?) to Quaternary (Houston and Dilles, 2013a). Zones of supergene copper oxides, including turquoise and chalcosiderite, occur with strong argillic alteration along the Continental fault and sporadically elsewhere (Eastman, 2017). Although Holocene age (<10,000 yr) normal faulting is widespread in western Montana, the scarps on the Continental and Rocker faults are degraded and vegetated and could be as old as Pleistocene (Houston and Dilles, 2013a). The record of normal faulting and supergene processes at Butte require further research.

PRESSURE AND TEMPERATURE IN THE BUTTE HYDROTHERMAL SYSTEM

In early studies of the EDM veins, Brimhall (1977) measured compositions of EDM K-feldspar by electron microprobe, then used those data with newly published experimental studies of Na-K partitioning in feldspars to determine that Butte EDM veinlets formed at temperatures in the range of 600°C to 700°C. Roberts (1973, 1975) constrained EDM temperature and pressure to approximately 600°C and 1.7–2.0 kb on the basis of his fluid inclusion measurements combined with mineral equilibria, especially the occurrence of muscovite–quartz–andalusite–K-feldspar in EDM alteration. The Roberts pressure estimate of ~2 kb (7 km) was a breakthrough in establishing what has since been recognized as a general maximum depth for porphyry copper deposit formation (Seedorff and others, 2005). Roberts based the pressure determination on measurements of Butte EDM fluid inclusions, which revealed abundant high-density inclusions (0.65 g/cm^3) whose pressure of trapping was 1.7 to 2.0 kb at an independently determined temperature of ~600°C.

Recent studies of Butte alteration mineral compositions, quartz fluid inclusions, and hornblende composition in the Butte Granite corroborate the findings of Roberts and Brimhall and extend P-T estimates to additional hydrothermal regimes such as those of pyrite//GS veins and Main Stage veins. Using three independent mineral thermobarometers, Ti-in-quartz, Zr-in-rutile, and Ti-in-biotite, Mercer and Reed (2013) estimate that the initial temperature of the magmatic-hydrothermal fluid that produced EDM veins was about 700°C and that the fluid entered host rock that was initially at ~450°C. This span of temperatures is reflected in the range of temperatures determined in quartz and rutile in single specimens, a span that captures the transient thermal state of the ascending fluids limited at the high end by the initial fluid temperature and at the low end by the initial wall-rock temperature deep in the deposit.

The 700°C to 450°C range applies to samples from biotite breccia, biotite crackles, EDM veins, and quartz–molybdenite veins. A majority of determined temperatures are 500°C to 650°C, over which range the effect of pressure on temperature estimates is modest, but the pressure effect is included in the temperature determinations based on a knowledge of fluid inclusions (see below). The titanium in biotite in alteration envelopes yields temperatures mostly between 600°C and 650°C. In contrast to the EDM and quartz–molybdenite veins, quartz and rutile temperatures in the pyrite//GS veins of the central GS zone are cooler—400°C to 550°C, with average temperatures ranging from 460°C to 510°C.

These vein temperature estimates can be combined with data from fluid inclusion measurements on all vein types by Rusk and others (2008a) to estimate pressure, as Roberts did (1975). The key pressure determination is based on the dominant deep fluid inclusions with ~35 vol.% bubbles (B35), that homogenize to liquid at ~360°C and have an average salinity of 5 wt% NaCl equivalent, and about 5 mol.% CO_2 (Rusk and others, 2008a). These inclusions are common in EDM veins where independent temperature estimates are 550 to 650°C, as described above, yielding a pressure of 2.0 kb to 2.5 kb, corresponding to lithostatic depths of 7 km to 9 km. Similar depths are indicated by hornblende geobarometry on unaltered granite surrounding Butte (Houston and Dilles, 2013a).

Rusk and others (2008a) also described B60 (60 vol.% bubble) fluid inclusions, which are common in the small amounts of quartz in the pyrite//GS veins of the central GS zone. GS fluid inclusions indicate temperatures in the range of 370°C to 450°C, the latter at a hydrostatic pressure of 700 kb, which indicates a hydrostatic depth of about 7 km at the time of GS vein formation. The GS fluid inclusion findings overlap the lower temperature end of those from Zr-in-rutile and Ti-in-quartz geothermometry (Mercer and Reed, 2013).

Fluid inclusions in Butte Main Stage vein quartz were examined by Miller (2004), Rusk and others (2008a, 2008b), and Ortelli (2015), who describe a dominant inclusion type with about 20 vol.% bubble, up to 2 mol.% CO_2, an average salinity of 3 wt% (range 1–6+ wt%) and homogenization to liquid at a temperature of 190° to 330°C (most at 240–310°C). Such salinities are consistent with mixtures of magmatic (4–6 wt% salinity) and meteoric fluids. Ortelli (2015) used pressure estimates of 60–220 b, consistent with hydrostatic pressures at ~750 m to 2.5 km depth, to estimate the Main Stage pressure-corrected trapping temperatures of ~200°C to 350°C.

CONCLUSION AND THE BUTTE METAL ENDOWMENT

Multiple events may have contributed to the cumulative ore endowment of the Butte District. The oldest rocks beneath the Boulder Batholith are metamorphic rocks of the 1.7 Ga Trans Montana orogenic belt (aka Big Sky Orogeny; USGS, 2007) overlain by sedimentary rocks of the 1.5–1.3 Ga Belt Supergroup. The latter were locally enriched in silver and base metals in the form of sedimentary-exhalative (SEDEX) and sediment-hosted stratiform copper deposits (Lydon, 2007). Much of the Belt-aged sediment-hosted sulfur was isotopically heavy, and could have been recycled into the Butte magmatic-hydrothermal system as suggested by Field and others (2005). The Cretaceous Butte Granite of the Boulder Batholith intruded Belt rocks and contains widespread ~75 Ma Ag-rich Pb-Zn (±Au-Cu-Mn) lodes that likely include some Main Stage ores in the western part of the Butte District (Lund and others, 2018).

The Butte ore system consists of two large porphyry Cu-Mo deposits centered on quartz porphyry dikes (fig. 15A): the eastern Pittsmont center (66 Ma), and the western Anaconda center (uncertain age of 66–64 Ma). These zones contain ~25 Mt of copper and as much as 2 Mt of molybdenum in ores deposited at ~500–700°C, and are cut by the large 64 Ma central GS quartz–sericite–pyrite zone. The younger ~350–200°C Main Stage veins (fig. 15B) are of uncertain age in the range of 64 to 62 Ma and include

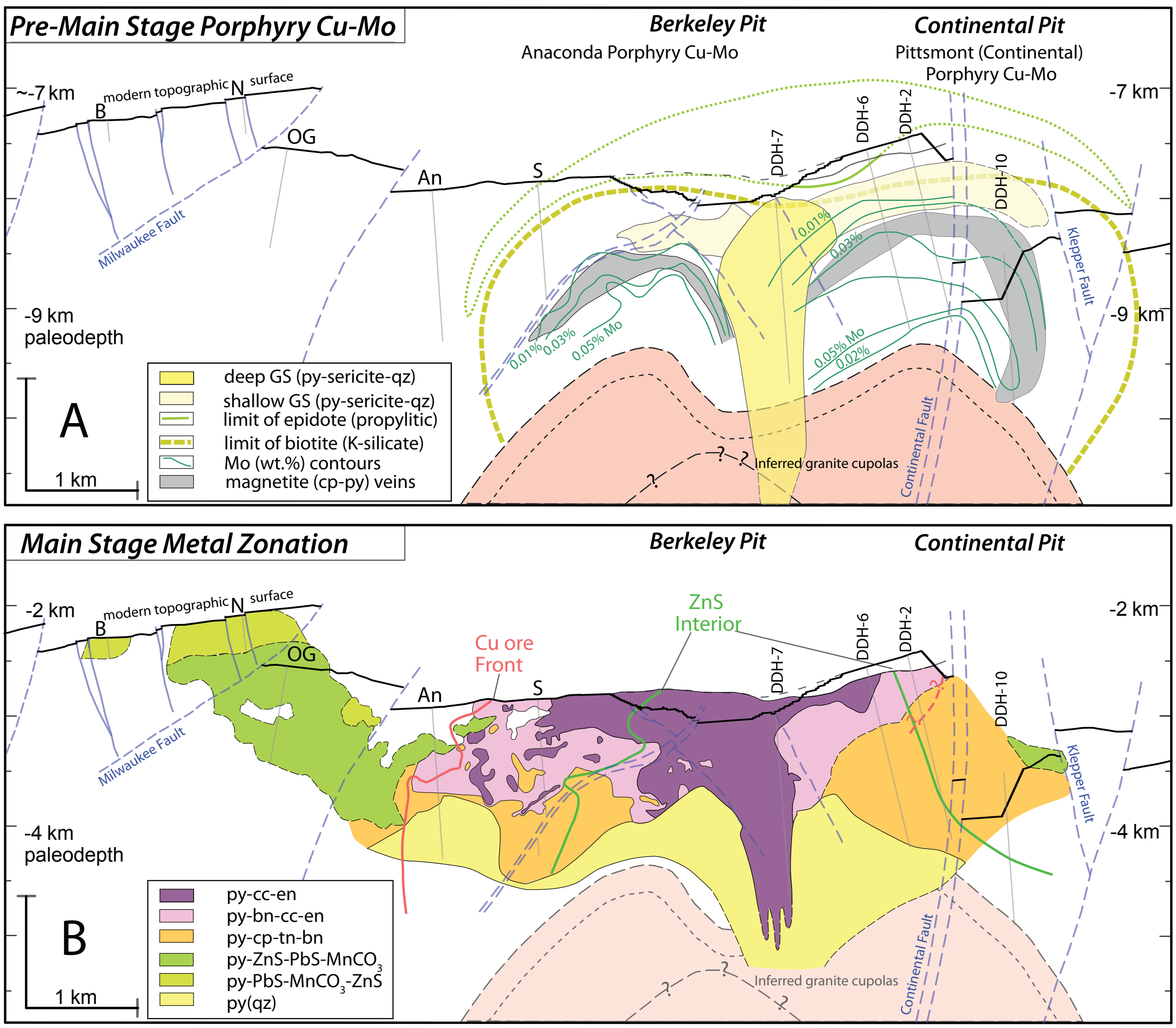

Figure 15. East–west cross section (A–A', see location fig. 3) through the Butte District, as restored to remove post-ore faults and tilting by Houston and Dilles (2012) and references therein. Gray lines in subsurface are the positions of several shafts and deep drillholes (DDH) that were used, together with other data, to construct the sections (A) Cross section illustrating restored configurations of pre-Main Stage Cu-Mo ores and alteration zones, with inferred cupolas sourcing the quartz porphyries. (B) Cross section illustrating restored distributions of the Main Stage metal zones (after Meyer and others, 1968; Proffett, 1979) with the Big Butte pyroclastic vent removed.

>10 Mt copper as well as Ag-Zn-Pb and Mn. Initial high temperature Main Stage ore fluids are similar in salinity and CO_2 concentration to the porphyry Cu-Mo magmatic-hydrothermal fluids, but at lower temperatures include an increasing proportion of meteoric water. Some Main Stage metals are remobilized from older porphyry Cu-Mo ores (Brimhall, 1978, 1979) and possibly from older ~75 Ma Ag-Pb-Zn veins, but most were newly introduced.

The various alteration assemblages on veins of the potassic series described above are consistent with formation from magmatic fluid of a single initial composition as it cooled and reacted with the granite wall rock; i.e. EDM, PGS, DGS, GS, and PRP alteration all form where an initial magmatic fluid resembling that in the B35 fluid inclusions reacts with Butte Granite over a range of temperatures and ratios of fluid to rock (water/rock ratio). This conclusion follows from a thermodynamics-based computation of the magmatic fluid reaction with granite (Reed and others, 2013).

The single-fluid reaction process produces feldspar-dominated alteration at the high temperatures of EDM veins, then the same fluid when cooled replaces feldspar with sericite in GS alteration at lower temperature. This effect is a result of disproportionation of abundant magmatic SO_2 to form hydrogen sulfide (H_2S) and sulfuric acid (H_2SO_4) as temperature drops from 700°C to 400°C (Ohmoto and Rye, 1979; Field and others, 2005). Reaction of the cooling fluid with wall-rock granite neutralizes the acid yielding PGS, DGS, GS, and propylitic assemblages at various temperatures and water/rock ratios. At lower temperature, the same fluid becomes quite acidic and is capable of producing the advanced argillic alteration and sericitic alteration of the Butte Main Stage.

The likelihood that the same fluid composition prevailed throughout mineralization, including deposition of barren quartz and quartz–molybdenite veins, is addressed by Reed and others (2013), drawing on ICP-MS measurements of fluid inclusions (Rusk and others, 2004, 2008a), now with added data from Ortelli (2015). The key finding from the fluid inclusions is that all vein types contain similar concentrations of salts and CO_2, except that in Main Stage fluids, salts, and CO_2 are slightly less concentrated, probably owing to dilution by meteoric waters.

ACKNOWLEDGMENTS

The world-class Butte Mining District holds a prominent place in geology not only for its enormous metal endowment but also because it yielded groundbreaking discoveries in hydrothermal geology through the insights of leading geologists Walter Weed, Reno Sales, and Charles Meyer.

Sales enabled the meticulous studies of mineralogy and chemical gains and losses in hydrothermally altered wall rock that Charles Meyer undertook in his Ph.D. research at Harvard University and in later studies at the University of California, Berkeley with his many students who worked on Butte: Julian Hemley, John Proffett, Steve Roberts, George Brimhall, Joe MacAleer, Ken Howard, Diane Wolfgram, Bob Page, and Mark Reed, plus Anaconda Company geologist George Burns. In all of his students, Meyer instilled an indelible understanding that sound conclusions about how nature works follow from accurate description of what is in the ground, starting from one's own mapping at every scale from microns to kilometers.

The authors thank Montana Resources for valued assistance in the form of financial support of students, access to core and geologic records, and insights from geologists George Burns, Steve Czehura, and Amanda Griffith. Anaconda sampler John Facincani provided invaluable technical assistance in data collection. Assistance from the Montana Bureau of Mines and Geology has been instrumental, especially from geologists Dick Berg and John Metesh, and administrative assistant Linda Albright. Former MBMG and Anaconda mineralogist Lester Ziehen contributed in the form of meticulous XRD measurements of alteration minerals and a generous endowment to maintain the collection of historic Butte rock specimens.

MR and JHD acknowledge financial support from National Science Foundation grants (JHD: EAR-9614683 & EAR-0001230; MHR: EAR-9704280, EAR-0001272, EAR- 0440198, EAR- 1524665), and the sponsors of the University of British Columbia-O.S.U. Porphyry Footprints Project.

The work of colleagues and students engaged in Oregon-based studies has been essential to our progress. Marisa Acosta, Federico Cernuschi, Sebastian Geiger, Scott Halley, Robert Houston, Celestine Mercer, Brooke Miller, Nansen Olson, Brian Rusk, Larry Snee, Holly Stein, Dick Tosdal, and Lihua Zhang have contributed data and thinking that were invaluable to this study. Critical reviews by C.H. Gammons and S. Czehura helped us clarify our presentation considerably.

REFERENCES

Acosta, M.D., Reed, M.H., and Watkins, J.M., 2017, The root of the Butte porphyry Cu deposit: A zone of fluid accumulation, discharge and collapse: American Geophysical Union Fall Meeting 2017, Abstract V51F-0422.

Acosta, M.D., Reed, M.H., and Watkins, J.M., 2018, Strain-induced quartz recrystallization in Butte porphyry Cu deposit produces mottled cathodoluminescent textures and preserves minimum Ti concentrations of dark euhedral bands: Goldschmidt Abstracts, 2018 12.

Acosta, M.D., Reed, M.H., and Watkins, J.M., 2019, Cathodoluminescent quartz textures reveal the importance of recrystallization in veins formed in the Butte porphyry Cu-Mo deposit, *in* Scarberry, K.C., and Barth, S., eds., Proceedings, Montana Mining and Mineral Symposium 2018: Montana Bureau of Mines and Geology Special Publication 120, p. 121–125.

Brecraft, G.E., Pinckney, D.M., and Rosenblum, S., 1963, Geology and mineral deposits of the Jefferson City quadrangle, Jefferson and Lewis and Clark Counties, Montana: U.S. Geological Survey Professional Paper 428, 101 p.

Brimhall, G.H., 1973, Mineralogy, texture, and chemistry of early wall rock alteration in the deep underground mines and Continental area, Butte district, Montana, *in* Miller, R.N., ed., Guidebook for the Butte field meeting of the Society of Economic Geologists: SEG Guidebook 1, The Anaconda Company, Butte, Montana, p. H1–H5.

Brimhall, G.H., Jr., 1977, Early fracture-controlled disseminated mineralization at Butte, Montana: Economic Geology, v. 72, p. 37–59.

Brimhall, G.H., Jr., 1978, Mechanisms of vein formation at Butte, Montana: Element recycling by hypogene leaching and enrichment of low-grade K-silicate protore: Economic Geology, v. 73, p. 1389.

Brimhall, G.H., Jr., 1979, Lithologic determination of mass transfer mechanisms of multiple-stage porphyry copper mineralization at Butte, Montana; vein formation by hypogene leaching and enrichment of potassium-silicate protore: Economic Geology, v. 74, p. 556–589.

Brimhall, G.H., Jr., and Ghiorso, M.S., 1983, Origin and ore-forming consequences of the advanced argillic alteration process in hypogene environments by magmatic gas contamination of meteoric fluids: Economic Geology, v. 78, p. 73–90.

Cathro, R.J., 2009, History: Butte Montana: CIM Magazine, parts 1–4: v. 4, no. 2, p. 69–71; no. 3, p. 81–83; no. 4, p. 69–72; no. 5, p. 73–75.

Christiansen, R.L., and Yeats, R.L., 1992, Post-Laramide geology of the U.S. Cordilleran region, *in* Burchfiel, B.C., Lipman, P.W., and Zoback, M.L., eds., The Cordilleran orogen: Conterminous U.S.: Geology of North America, v. G-3: Boulder, Colo., Geological Society of America, p. 261–406.

Czehura, S.J., 2006, Butte, a world class ore deposit: Mining Engineering, v. 58, p. 14–19.

DeWitt, E., Foord, E.E., Zartman, R.E., Pearson, R.C., and Foster, F., 1996, Chronology of Late Cretaceous igneous and hydrothermal events at the Golden Sunlight gold–silver breccia pipe, southwestern Montana: U.S. Geological Survey Bulletin 2155.

Dilles, J.H., Reed, M.H., Roberts, S., Zhang, L., and Houston, R., 1999, Early magmatic-hydrothermal features related to porphyry copper mineralization at Butte: Montana Geological Society of America Abstracts with Programs, v. 31, no. 7, p. A-380.

Dilles, J., Reed, M., Rusk, B., Houston, R., Zhang, L., Martin, M., Snee, L., Stein, H., Field, C., and Kent, A., 2006, Lessons from Butte, Montana: Exploration and mining applications from recent research: Society of Economic Geologists, Business of Exploration Meeting, Keystone, Colo., 2006, Extended abstract, 4 p.

Dilles, J., Stein, H., Martin, M., and Rusk B., 2004, Re-Os and U-Pb ages for the Butte copper district, Montana: International Association of Volcanology and Chemistry of the Earth's Interior (IAVCEI) Meeting, Púcon, Chile, 14–19 November 2004, Proceedings, 1 p.

du Bray, E.A., Aleinikoff, J.N., and Lund, K., 2012, Synthesis of petrographic, geochemical, and isotopic data for the Boulder Batholith, southwest Montana: U.S. Geological Survey Professional Paper 1793, 39 p.

Dudás, F., Ispolatov, V., Harlan, S., and Snee, L., 2010, ^{40}Ar/^{39}Ar geochronology and geochemical reconnaissance of the Eocene Lowland Creek Volcanic Field, west-central Montana: Journal of Geology, v. 118, no. 3, p. 295–304.

Eastman, K., 2017, Supergene mineralization of the Continental Pit, Butte, Silver Bow County, Montana: Butte, Montana Tech, M.S. thesis, 199 p., available at https://digitalcommons.mtech.edu/grad_rsch/125/ [Accessed August 2020].

Emmons, S., and Tower, G., 1897, Economic geology of the Butte special district (Montana): U.S. Geological Survey Geologic Atlas of the United States, Butte Folio, no. 38, p. 3–8.

English, J., Johnston, S., and Wang, K., 2003, Thermal modeling of the Laramide orogeny: Testing the flat-slab subduction hypothesis: Earth and Planetary Science Letters, v. 214, p. 619–632.

Field, C.W., Zhang, L., Dilles, J.H., Rye, R.O., and Reed, M.H., 2005, Sulfur and oxygen isotope record in sulfate and sulfide minerals of early, deep, pre-Main Stage porphyry Cu-Mo and late Main Stage base-metal mineral deposits, Butte district, Montana: Chemical Geology, v. 215, p. 61–93.

Foster, D., Warren, G., Jr., and Kalakay, T., 2010, Extension of the Anaconda metamorphic core complex: ^{40}Ar/^{39}Ar thermochronology and implications for Eocene tectonics of the northern Rocky Mountains and the Boulder Batholith: Lithosphere, v. 2, p. 232–246.

Gammons, C.H., Szarkowski, J., and Stevenson, R., 2016, New investigations of the mineralogy of silver in the world-class porphyry-lode deposits of Butte, Montana: Mineral Engineering v. 2–8, June 2016, available at http://me.smenet.org/docs/Publications/ME/Issue/WebExclusiveFinal.pdf [Accessed August 2020].

Gammons, C.H., and Duaime, T.E., 2020, The Berkeley Pit and surrounding mine waters of Butte, *in* Metesh, J.J., and Gammons, C.H., eds., Geology of Montana—Special Topics: Montana Bureau of Mines and Geology Special Publication 122: v. 2, 17 p.

Gammons, C.H., Korzeb, S., and Hargrave, P., 2020, Metallic ore deposits of Montana, *in* Metesh, J.J., and Gammons, C.H., eds., Geology of Montana—Special Topics: Montana Bureau of Mines and Geology Special Publication 122: v. 2, 30 p.

Garlick, G.D., and Epstein, S., 1966, The isotopic composition of oxygen and carbon in hydrothermal minerals from Butte, Montana: Economic Geology, v. 61, p. 1325–1335.

Geissman, J., Van Der Voo, R., Kelly, W., and Brimhall, G., Jr., 1980a, Paleomagnetism, rock magnetism, and aspects of structural deformation of the Butte mining district, Butte, Montana: Journal of Geology, v. 88, p. 129–159.

Geissman, J., Van Der Voo, R., Kelly, W., and Brimhall, G., Jr., 1980b, Paleomagnetic documentation of the early, high-temperature zone of mineralization at Butte, Montana: Economic Geology, v. 75, p. 1210–1219.

Giggenbach, W., 1997, The origin and evolution of fluids in magmatic-hydrothermal systems, *in* Barnes, H.L., ed., Geochemistry of hydrothermal ore deposits, 3rd ed.: New York, John Wiley, p. 737–796.

Gilg, H.A., and Sheppard, S.M.F., 1996, Hydrogen isotope fractionation between kaolinite and water revisited: Geochimica et Cosmochimica Acta, v. 60, p. 529–533.

Guilbert, J.M., and Zeihen, L.G., 1964, The mineralogy of the Butte district, Montana: Proceedings of the Northwest Mining Association, Spokane, Washington, December 1964.

Gustafson, D., 1973, Distribution, mineralogy, and structural features of the horsetail zones, Butte district, Montana, *in* Miller, R., ed., Guidebook for the Butte field meeting of the Society of Economic Geologists: SEG Guidebook 1, The Anaconda Company, Butte, Montana, p. J1–J5.

Harris, A.C., and Golding, S.D., 2002, New evidence of magmatic-fluid–related phyllic alteration: Implications for the genesis of porphyry Cu deposits: Geology, v. 30, p. 335–338.

Houston, R.A., and Dilles, J.H., 2013a, Structural geologic evolution of the Butte District, Montana: Economic Geology: v. 108, p. 1397–1424.

Houston, R.A., and Dilles, J.H., 2013b, Geology of the Butte mining district, Montana: Montana Bureau of Mines and Geology Open-File Report 627, 1 sheet, scale 1:24,000.

Kalakay, T., John, B., and Lageson, D., 2001, Fault-controlled pluton emplacement in the Sevier fold-and-thrust belt of southwest Montana, USA: Journal of Structural Geology, v. 23, p. 1151–1165.

Lageson, D.R., Schmitt, J.G., Horton, B.K., Kalakay, T.J., and Burton, B.R., 2001, Influence of Late Cretaceous magmatism on the Sevier orogenic wedge, western Montana: Geology, v. 29, no. 8, p. 723–726.

Lange, I.M., and Cheney, E.S., 1971, Sulfur isotope reconnaissance of Butte, Montana: Economic Geology, v. 66, p. 63–74.

Long, K.R., 1995, Production and reserves of Cordilleran (Alaska to Chile) porphyry copper deposits, *in* Pierce, F., and Bolm, J., eds., Porphyry copper deposits of the American Cordillera: Arizona Geological Society Digest, v. 20, p. 35–68.

Long, K.R., DeYoung, J.H., and Ludington, S., 2000, Significant deposits of gold, silver, copper, lead, and zinc in the United States: Economic Geology, v. 95, p. 629–644.

Lund, K., Aleinikoff, J., Kunk, M., Unruh, D., Zeihen, G., Hodges, W., Du Bray, E., and O'Neill, J., 2002, SHRIMP U-Pb and $^{40}Ar/^{39}Ar$ age contrasts for relating plutonism and mineralization in the Boulder Batholith region, Montana: Economic Geology, v. 97, p. 241–267.

Lund, K., Aleinikoff, J.N., Kunk, M.J., and Unruh, D.M., 2007, SHRIMP U-Pb and $^{40}Ar/^{39}Ar$ age constraints for relating plutonism and mineralization in the Boulder Batholith region, Montana, *in* Lund, K., ed., Earth Science studies in support of Public Policy Development and Land Stewardship—Headwaters Province, Idaho and Montana: U.S. Geological Survey Circular 1305, p. 39–48, available at http://pubs.usgs.gov/circ/1305/ [Accessed August 2020].

Lund, K., McAleer, R.J., Aleinikoff, J.N., Cosca, M.A., and Kunk, M.J., 2018, Two-event lode-ore deposition at Butte, USA: $^{40}Ar/^{39}Ar$ and U-Pb documentation of Ag-Au-polymetallic lodes overprinted by younger stockwork Cu-Mo ores and penecontemporaneous Cu lodes: Ore Geology Reviews, v. 102, p. 666–700.

Lydon, J.W., 2007, Geology and metallogeny of the Belt–Purcell Basin: Geological Association of Canada Mineral Deposits Division, p. 581–607.

Mahoney, J.B., Pignotta, G.S., Ihinger, P.D., Wittkop, C., Balgord, E.A., Potter, J.J., and Leistikow, A., 2015, Geologic relationships in the northern Helena salient, Montana: Northwest Geology, v. 44, p. 109–136.

Malone, M.P., 1981, The battle for Butte: Mining and politics on the northern frontier, 1864–1906: Seattle, University of Washington Press (reprinted in 1995 by the Montana Historical Society Press, Helena).

Martin, M.W., Dilles, J., and Proffett, J.M, 1999, U-Pb geochronologic constraints for the Butte porphyry system [abstract]: Geological Society of America Abstracts with Programs, v. 31, no. 7, p. A380.

Martin, M., and Dilles, J.H., 2000, U-Pb zircon and sphene geochronologic constraints for the Butte porphyry system: Geological Society of America Abstracts with Programs, v. 32, no. 6, p. A28.

McClave, M.A., 1973, Control and distribution of supergene enrichment in the Berkeley Pit, Butte district, Montana, *in* Miller, R., ed., Guidebook for the Butte field meeting of the Society of Economic Geologists: SEG Guidebook 1, The Anaconda Company, Butte, Montana, p. K1–K4.

Mercer, C., and Reed, M., 2013, Porphyry Cu-Mo stockwork formation by dynamic, transient hydrothermal pulses: Mineralogic insights from the deposit at Butte, Montana: Economic Geology, v. 108, p. 1347–1377.

Mercer, C., Reed, M., and Mercer, C., 2015, Time-scales of porphyry Cu deposit formation: Insights from titanium diffusion in quartz: Economic Geology, v. 110, p. 587–602.

Meyer, C., 1965, An early potassic type of wall rock alteration at Butte, Montana: American Mineralogist, v. 50, p. 1717–1722.

Meyer, C., and Hemley, J.J., 1967, Wall rock alteration, *in* Barnes, H.L., ed., Geochemistry of hydrothermal ore deposits: New York, Holt, Rinehart and Winston, Inc., p. 166–232.

Meyer, C., Shea, E., Goddard, C., and staff, 1968, Ore deposits at Butte, Montana, *in* Ridge, J.D., ed., Ore deposits of the United States 1933–1967, The Graton-Sales Volume: New York, American Institute of Mining, Metallurgical, and Petroleum Engineers, v. 2, p. 1363–1416.

Miller, B.J., 2004, Aqueous fluid inclusions in the

Butte, Montana, Main Stage vein system: Eugene, University of Oregon, M.S. thesis, 101 p.

Miller, R.N., 1973, Production history of the Butte district, and geological function, past and present, *in* Miller, R., ed., Guidebook for the Butte field meeting of the Society of Economic Geologists: SEG Guidebook 1, The Anaconda Company, Butte, Montana, p. F-1 to F-10.

Minervini, G., 1975, Quartz porphyry intrusions and associated propylitic breccias in the Modoc area, Butte district, Montana: Butte, Montana Technological University, 55 p.

Mosolf, J.G., Kalakay, T.J., and Foster, D.A., 2020, Eocene magmatism and coeval crustal extension in Montana, *in* Metesh, J.J., and Vuke, S.M., eds., Geology of Montana—Geologic History: Montana Bureau of Mines and Geology Special Publication 122, v. 1.

Mueller, P.A., Heatherington, A.L., Kelly, D.M., Wooden, J.L., and Mogk, D.W., 2002, Paleoproterozoic crust within the Great Falls tectonic zone: Implications for the assembly of southern Laurentia: Geology, v. 30, p. 127–130.

Naney, M.T., 1983, Phase equilibria of rock-forming ferromagnesian silicates in granitic systems: American Journal of Science, v. 283, p. 993–1033.

Ohmoto, H., and Rye, R.O., 1979, Isotopes of sulfur and carbon, *in* Barnes, H.L., ed., Geochemistry of hydrothermal ore deposits, 2nd ed.: New York, John Wiley, p. 509–567.

Olson, N.H., Dilles, J.H., Kallio, I.M., Horton, T.R., and Scarberry, K.C., 2016, Geologic map of the Ratio Mountain 7.5' quadrangle, southwest Montana: Montana Bureau of Mines and Geology EDMAP 10, 1:24,000.

Olson, N.H., Sepp, M.D., Mankins, N.E., Blessing, J.M., Dilles, J.H., and Scarberry, K.C., 2017, Geologic map of the Mount Thompson 7.5' quadrangle, southwest Montana: Montana Bureau of Mines and Geology EDMAP 11, scale 1:24,000.

O'Neill, J.M., and Lopez, D.A., 1985, The Great Falls tectonic zone—Its character and regional significance: American Association of Petroleum Geologists Bulletin, v. 69, p. 437–447.

Ortelli, M., 2015, Chemistry and physical properties of ore-forming fluids trapped in ore and gangue minerals: New insights into mineralization processes in magmatic-hydrothermal systems with special focus on the Butte Mining District (USA): Switzerland, University of Geneva, Ph.D. dissertation.

Ortelli, M., Kouzmanov, K., Dilles, J.H., and Rusk, B.G., 2013, District-scale fluid evolution in the Main Stage veins at Butte, Montana, *in* Deposit research for a high-tech world: Proceedings, 12th SGA Biennial Meeting, 2013.

Ortelli, M., Kouzmanov, K., Walle, M., and Dilles, J.H., 2015, Comparative study of fluid inclusions trapped in cogenetic ore and gangue minerals: Mineral resources in a sustainable world: 13th SGA Biennial Meeting 2015 Proceedings, v. 2.

Oyer, N., Childs, J., and Mahoney, J.B., 2014, Regional setting and deposit geology of the Golden Sunlight Mine: An example of responsible resource extraction, *in* Shaw, C.A., and Tikoff, B., eds., Exploring the Northern Rocky Mountains: Geological Society of America Field Guide, v. 37, p. 115–144.

Page, R., 1979, Alteration-mineralization history of the Butte, Montana ore deposit, and transmission electron microscopy of phyllosilicate alteration phases: Berkeley, University of California, Ph.D. thesis, 226 p.

Parry, W.T., 2004, All veins, lodes, and ledges throughout their entire depth: Geology and the apex law in Utah mines: Salt Lake City, The University of Utah Press.

Proffett, J.M., 1973, Structure of the Butte district, Montana, *in* Miller, R., ed., Guidebook for the Butte field meeting of the Society of Economic Geologists: SEG Guidebook 1, The Anaconda Company, Butte, Montana, p. G-1 to G-12.

Proffett, J.M., 1979, Ore deposits of the western United States—A summary, *in* Ridge, J., ed., Papers on mineral deposits of western North America—The International Association on the Genesis of Ore Deposits Fifth Quadrennial Symposium: Nevada Bureau of Mines and Geology Report 33, p. 13–32.

Proffett, J.M., Burns, G., and Anaconda staff, 1982, Geologic map of the Butte district, Montana: Anaconda Archives, American Heritage Museum, Laramie, Wyo., scale 1:12,000.

Proffett, J.M., and Burns, G., 1999, Tilting in the Butte district, Montana, and possible implications for interpretation of metal zoning: Geological Society of America Abstracts with Programs, v. 31, no. 7, p. 382.

Reed, M.H., 1979, Butte district early stage geology synthesis: Unpublished Anaconda Company Report, 42 p.

Reed, M.H., 1980, Distribution of mineralization at Butte, an addendum: Unpublished Anaconda Company Report, 25 p.

Reed, M.H., 1981, Summary of recent developments in the interpretation of Butte geology: Unpublished Anaconda Company Report, 28 p.

Reed, M.H., 1994, Hydrothermal alteration in active continental hydrothermal systems, *in* Lentz, D.R., ed., Alteration and alteration processes associated with ore-forming systems: Geological Association of Canada Short Course Notes, v. 11, p. 315–337.

Reed, M., and Palandri, J., 2006, Sulfide mineral precipitation from hydrothermal fluids: Reviews in mineralogy and geochemistry, v. 60: Sulfide mineralogy and geochemistry, ch. 11, p. 609–632.

Reed, M.H., Rusk, B., and Palandri, J., 2013, The Butte magmatic-hydrothermal system: One fluid yields all alteration and veins: Economic Geology, v. 108, p. 1379–1396.

Roberts, S.A., 1973, Pervasive early alteration in the Butte district, Montana, *in* Miller, R.N., ed., Guidebook for the Butte field meeting of the Society of Economic Geologists: SEG Guidebook 1, The Anaconda Company, Butte, Montana, p. HH1–HH8.

Roberts, S., 1975, Early hydrothermal alteration and mineralization in the Butte district, Montana: Harvard University, Ph.D. dissertation, 157 p.

Rusk, B.G., and Reed, M.H., 2002, Scanning electron microscope-cathodoluminescence analysis of quartz reveals complex growth histories in veins from the Butte porphyry copper deposit, Montana: Geology, v. 30, p. 727–730.

Rusk, B., Reed, M., Dilles, J.H., Klemm, L., and Heinrich, C.A., 2004, Compositions of magmatic hydrothermal fluids determined by LA-ICP-MS of fluid inclusions from the porphyry copper-molybdenum deposit at Butte, Montana: Chemical Geology, v. 210, p. 173–199.

Rusk, B., Reed, M., and Dilles, J., 2008a, Fluid inclusion evidence for magmatic-hydrothermal fluid evolution in the porphyry copper–molybdenum deposit at Butte, Montana: Economic Geology, v. 103, p. 307–334.

Rusk, B.G., Miller, B.J., and Reed, M.H., 2008b, Fluid inclusion evidence for the formation of main stage polymetallic base-metal veins, Butte, Montana, USA: Tucson, Arizona Geological Society Digest, v. 22, p. 573–581.

Rutland, C., Smedes, H., Tilling, R., and Greenwood, W., 1989, Volcanism and plutonism at shallow crustal levels: The Elkhorn Mountains Volcanics and the Boulder Batholith, southwestern Montana, *in* Henshaw, P., ed., Volcanism and plutonism of western North America; v. 2, Cordilleran volcanism, plutonism, and magma generation at various crustal levels, Montana and Idaho, Field trips for the 28th International Geological Congress: American Geophysical Union, Monograph, p. 16–31.

Sales, R.H., 1914, Ore deposits at Butte, Montana: Transactions of the American Institute of Mining, Metallurgical and Petroleum Engineers, v. 46, p. 3–109.

Sales, R.H., 1964, Underground warfare at Butte: Caldwell, Idaho: Caxton Printers, Ltd.

Sales, R., and Meyer, C., 1948, Wall rock alteration at Butte: American Institute of Mining and Metallurgical Engineers, Transactions, v. 46, p. 4–106.

Sales, R., and Meyer, C., 1949, Results from preliminary studies of vein formation at Butte, Montana: Economic Geology, v. 44, p. 465–484.

Scarberry, K.C., Yakovlev, P.V., and Schwartz, T.M., 2020, Mesozoic Magmatism in Montana, *in* Metesh, J.J., and Vuke, S.M., eds., Geology of Montana—Geologic History: Montana Bureau of Mines and Geology Special Publication 122, v. 1.

Sears, J., 2001, Emplacement and denudation history of the Lewis–Eldorado–Hoadley thrust slab in the northern Montana Cordillera, USA: Implications for steady-state orogenic processes: American Journal of Science, v. 301, p. 359–373.

Seedorff, E., Dilles, J.H., Proffett, J.M., Einaudi, M.T., Zurcher, L., Stavast, W.J.A., Johnson, D.A., and Barton, M.D., 2005, Porphyry deposits: Characteristics and origin of hypogene features: Economic Geology, 100th Anniversary Volume, p. 251–298.

Seedorff, E., and Einaudi, M., 2004, Henderson porphyry molybdenum system, Colorado. I. Sequence and abundance of hydrothermal mineral assemblages, flow paths of evolving fluids, and evolutionary style: Economic Geology, v. 99, p. 3−37.

Sharp Z.D., Gibbons, J.A., Maltsev, O., Atudorei, V., Pack, A., Sengupta, S., Shock, E.L., and Knauth, L.P., 2016, A calibration of the triple oxygen isotope fractionation in the SiO_2-H_2O system and applications to natural samples: Geochimica et Cosmochimica Acta, v. 186, p. 105–119.

Sheppard, S.M.F., Nielsen, R.L., and Taylor, H.P., Jr., 1969, Oxygen and hydrogen isotope ratios of clay minerals from porphyry copper deposits: Economic Geology, v. 64, p. 755–777.

Sheppard, S.M.F., Nielsen, R.L., and Taylor, H.P., Jr., 1971, Hydrogen and oxygen isotope ratios in minerals from porphyry copper deposits: Economic Geology, v. 66, p. 515–542.

Sheppard, S.M.F., and Taylor, H.P., 1974, Hydrogen and oxygen isotope evidence for the origins of water in the Boulder Batholith and the Butte ore deposits, Montana: Economic Geology, v. 69, p. 926–946.

Sillitoe, R.H., 1973, The tops and bottoms of porphyry copper deposits: Economic Geology, v. 68, p. 799–815.

Sillitoe, R.H., 2010, Porphyry copper systems: Economic Geology, v. 105, p. 3–41.

Sillitoe, R.H., Grauberger, G.L., and Elliott, J.E., 1985, A diatreme-hosted gold deposit at Montana Tunnels, Montana, Economic Geology, v. 80, p. 1707–1721.

Simmons, S.F., White, N.C., and John, D.A., 2005, Geologic characteristics of epithermal precious and base metal deposits, *in* Hedenquist, J.W., Thompson, J.F.H., Goldfarb, R.J., and Richards, J.P., eds.: Economic Geology 100th Anniversary Volume, p. 451–484.

Smedes, H.W., 1962, Lowland Creek Volcanics, an Upper Oligocene formation near Butte, Montana: The Journal of Geology, v. 70, p. 255–266.

Smedes, H.W., 1966, Geology and igneous petrology of the northern Elkhorn Mountains, Jefferson and Broadwater counties, Montana: U.S. Geological Survey Professional Paper 510, 116 p.

Smedes, H.W., Klepper, M.R., and Tilling, R.I., 1973, The Boulder Batholith, Montana, A summary, *in* Miller, R.N., ed., Guidebook for the Butte field meeting of the Society of Economic Geologists: SEG Guidebook 1, The Anaconda Company, Butte, Montana, p. E1–E16.

Smedes, H., Klepper, M., and Tilling, R., 1988, Preliminary map of plutonic units of the Boulder Batholith, southwestern Montana: Montana Bureau of Mines and Geology Open-File Report 88-283, scale 1:200,000 (and digital reprinted USGS Data Series 454, 2009).

Snee, L., Miggins, D., Geissman, J., Reed, M., Dilles, J., and Zhang, L., 1999, Thermal history of the Butte porphyry system, Montana [abstract]: Geological Society of America Abstracts with Program, v. 31, p. 380.

Spear, F.S., 1993, Metamorphic phase equilibria and pressure–temperature–time paths: Mineralogical Society of America, Washington DC, 799 p.

Stevenson, R., 2015, Stable isotopes of hydrothermal carbonate minerals in the Butte porphyry-lode deposits, Montana: Butte, Montana Technological University, M.S. thesis, 84 p., available at https://digitalcommons.mtech.edu/grad_rsch/44/ [Accessed August 2020].

Sverjensky, D.A., Hemley, J.J., and d'Angelo, W.M., 1991, Thermodynamic assessment of hydrothermal alkali feldspar–mica–aluminosilicate equilibria: Geochimica et Cosmochimica Acta, v. 55, p. 989–1004.

Taylor, H.P., 1979, Oxygen and hydrogen isotope relationships in hydrothermal mineral deposits, *in* Barnes, H.L., ed., Geochemistry of hydrothermal ore deposits, 2nd ed.: New York, John Wiley, p. 236–277.

Taylor, H.P., 1997, Oxygen and hydrogen isotope relationships in hydrothermal mineral deposits, *in* Barnes, H.L., ed., Geochemistry of hydrothermal ore deposits, 3rd ed.: New York, John Wiley, p. 229–302.

Thompson, B., 1973, Distribution of primary mineralization and hydrothermal alteration within the Berkeley Pit, Butte district, Montana, *in* Miller, R.N., ed., Guidebook for the Butte field meeting of the Society of Economic Geologists: SEG

Guidebook 1, The Anaconda Company, Butte, Montana, p. G1–G7.

Tilling, R.I., 1964, Variation in modes and norms of an "Homogeneous" pluton of the Boulder Batholith, Montana: U.S. Geological Survey Professional Paper 501-D, p. D8–D13.

Tilling, R.I., 1973, Boulder Batholith, Montana—A product of two contemporaneous but chemically distinct magma series: Geological Society of America Bulletin, v. 84, p. 3879–3900.

Tilling, R.I., 1974, Composition and time relations of plutonic and associated volcanic rocks, Boulder Batholith region, Montana: Geological Society of America Bulletin, v. 85, p. 1925–1930.

Tosdal, R.M., and Dilles, J.H., in press, Creation of permeability in the porphyry Cu environment, *in* Rowland, J., and Rhys, D., eds., Structural Geology: Reviews in Economic Geology, Society of Economic Geologists.

U.S. Geological Survey Headwaters Province Project Team (Karen Lund, scientific ed.), 2007, Earth science studies in support of public policy development and land stewardship—Headwaters province, Idaho and Montana: U.S. Geological Survey Circular 1305, 92 p.

Vennemann, T.W., and O'Neil, J.R., 1996, Hydrogen isotope exchange reactions between hydrous minerals and molecular hydrogen. I. A new approach for the determination of hydrogen isotope fractionation at moderate temperatures: Geochimica et Cosmochimica Acta, v. 60, p. 2437–2451.

Weed, W.H., 1897, Description of the Butte Special District: U.S. Geological Survey, Geologic Atlas of the United States, Butte Folio, no. 38, p. 1–3.

Weed, W.H., 1912, Geology and ore deposits of the Butte district, Montana: U.S. Geological Survey Professional Paper 74, p. 3–57.

Wightman, E., 1979, Butte aeromagnetic and gravity surveys: Anaconda Company Report.

Zhang, L., 2000, Stable isotope investigation of a hydrothermal alteration system: Butte porphyry copper deposit: Corvallis, Oregon State University, unpublished Ph.D. thesis, 182 p.

Zhang, L., Dilles, J.H., Field, C.W., and Reed, M.H., 1999, Oxygen and hydrogen isotope geochemistry of pre-main stage porphyry Cu-Mo mineralization at Butte, Montana: Geological Society of America Abstracts with Programs, v. 31, no. 7, p. A381.

Zheng, Y-F., 1993, Calculation of oxygen isotope fractionation factors in hydroxyl-bearing silicates: Earth Planetary Science Letters, v. 120, p. 243–263.